Agricultural and Forest Meteorology 259 (2018) 329–344

Contents lists available at ScienceDirect

Agricultural and Forest Meteorology

journal homepage: www.elsevier.com/locate/agrformet

Climate shifts within major agricultural seasons for +1.5 and +2.0 °C worlds: HAPPI projections and AgMIP modeling scenarios

Alex C. Ruane[a,*], Meridel M. Phillips[a,b], Cynthia Rosenzweig[a]

[a] NASA Goddard Institute for Space Studies, New York, NY, USA
[b] Columbia University Earth Institute Center for Climate Systems Research, New York, NY, USA

ARTICLE INFO

Keywords:
Climate change
Climate impacts
Agricultural impacts
AgMIP
HAPPI
Paris Agreement

ABSTRACT

This study compares climate changes in major agricultural regions and current agricultural seasons associated with global warming of +1.5 or +2.0 °C above pre-industrial conditions. It describes the generation of climate scenarios for agricultural modeling applications conducted as part of the Agricultural Model Intercomparison and Improvement Project (AgMIP) Coordinated Global and Regional Assessments. Climate scenarios from the Half a degree Additional warming, Projections, Prognosis and Impacts project (HAPPI) are largely consistent with transient scenarios extracted from RCP4.5 simulations of the Coupled Model Intercomparison Project phase 5 (CMIP5). Focusing on food and agricultural systems and top-producing breadbaskets in particular, we distinguish maize, rice, wheat, and soy season changes from global annual mean climate changes. Many agricultural regions warm at a rate that is faster than the global mean surface temperature (including oceans) but slower than the mean land surface temperature, leading to regional warming that exceeds 0.5 °C between the +1.5 and +2.0 °C Worlds. Agricultural growing seasons warm at a pace slightly behind the annual temperature trends in most regions, while precipitation increases slightly ahead of the annual rate. Rice cultivation regions show reduced warming as they are concentrated where monsoon rainfall is projected to intensify, although projections are influenced by Asian aerosol loading in climate mitigation scenarios. Compared to CMIP5, HAPPI slightly underestimates the CO_2 concentration that corresponds to the +1.5 °C World but overestimates the CO_2 concentration for the +2.0 °C World, which means that HAPPI scenarios may also lead to an overestimate in the beneficial effects of CO_2 on crops in the +2.0 °C World. HAPPI enables detailed analysis of the shifting distribution of extreme growing season temperatures and precipitation, highlighting widespread increases in extreme heat seasons and heightened skewness toward hot seasons in the tropics. Shifts in the probability of extreme drought seasons generally tracked median precipitation changes; however, some regions skewed toward drought conditions even where median precipitation changes were small. Together, these findings highlight unique seasonal and agricultural region changes in the +1.5 °C and +2.0 °C worlds for adaptation planning in these climate stabilization targets.

1. Introduction

Changes in the Earth's climate present an array of challenging consequences for humankind in the coming decades (IPCC, 2013). Food systems, in particular, are at risk from rising temperatures, droughts, floods, and extreme events (Beddington et al., 2012; Porter et al., 2014; Brown et al., 2015; FAO, 2016). In light of observed and projected impacts, representatives of 196 parties signed the United Nations Framework Convention on Climate Change (UNFCCC) Paris Agreement (UNFCCC, 2015) in December 2015, agreeing to pursue efforts that would limit the global mean surface temperature increase to 2 °C above pre-industrial temperature levels, with ambition to limit the rise below +1.5 °C (both would require substantial deviation from the current business-as-usual greenhouse gas emission pathway). These commitments do not eliminate anthropogenic climate change or the need to sustainably adapt natural and human systems, but seek to diminish the risk of increasingly dangerous impacts associated with more extreme climate changes (IPCC, 2014).

The Paris Agreement is largely focused on major policy and technological issues related to how climate change may be mitigated, but has also given rise to the scientific question: What type of world would be achieved should efforts to mitigate greenhouse gas emissions and land use change be successful at keeping the world at either +1.5 °C or +2.0 °C above pre-industrial temperature levels? Answers to this

* Corresponding author at: NASA Goddard Institute for Space Studies, 2880 Broadway, New York, NY, 10025, USA.
E-mail address: alexander.c.ruane@nasa.gov (A.C. Ruane).

https://doi.org/10.1016/j.agrformet.2018.05.013
Received 31 October 2017; Received in revised form 22 April 2018; Accepted 12 May 2018
Available online 01 June 2018
0168-1923/ Published by Elsevier B.V.

question are aided by the creation and analysis of hypothetical climate states stabilized at +1.5 °C and +2.0 °C above pre-industrial conditions, hereafter referred to as the '+1.5 °C World' and '+2.0 °C World'. These projections allow us to compare future and current conditions and evaluate potentially beneficial or detrimental climate impacts across regions, sectors, and populations. These impacts, the resulting need for adaptation, and pressure on current land use patterns must be considered along with the costs of mitigation in determining future societal pathways and climate targets.

Here we describe likely challenges for the agricultural sector under +1.5 and +2.0 °C Worlds, identifying key characteristics of projected changes for current growing seasons in major breadbaskets. Agro-climatic indicators may contribute to more efficient adaptation interventions in the agricultural sector, potentially including shifts in planting date, seed varieties, irrigation applications, crop insurance, farm systems, food value chains, and the management of pests, diseases, and weeds (Howden et al., 2007; Rosenzweig and Tubiello, 2007; Yadav et al., 2011; Rickards and Howden, 2012).

The agro-climatic projections serve as the driving conditions for agricultural model analyses utilizing protocols developed within the Agricultural Model Intercomparison and Improvement Project (AgMIP; Rosenzweig et al., 2013, 2014, 2015; Ruane et al., 2017). In particular, AgMIP's Coordinated Global and Regional Assessments (CGRA) utilize a simulation framework linking biophysical and economic impacts on global and local scales to consistently evaluate the impacts of climate, socioeconomic development, and policy scenarios on agriculture and food security (Rosenzweig et al., 2016, 2018; Ruane et al., 2018). CGRA analyses of the +1.5 and +2.0 °C Worlds are thus grounded in climate scenarios with consistent methodologies and assumptions, allowing CGRA findings to focus on emergent cross-disciplinary and cross-scale findings.

2. Methodology

The targets of +1.5 and +2.0 °C global warming, here defined as global increase in average near-surface air temperature above pre-industrial conditions, are dependent on the selection of a pre-industrial period that was not explicitly delineated by the UNFCCC. A number of pre-industrial period definitions have been utilized in prior Intergovernmental Panel on Climate Change (IPCC) assessments (IPCC et al., 2013, 2014; Clarke et al., 2014), some pegging it to the early industrial period starting in 1760 or more often connecting it to the 1850–1900 period (which is also the beginning of historical period climate simulations; Taylor et al., 2012). Historical station-based temperature datasets are available beginning in 1850 (Hadley Center Climate Research Unit Temperature, HadCRUT4, Morice et al., 2012; Berkeley Earth Surface Temperature, BEST, Rohde et al., 2013), with additional datasets available by the 1880–1900 period (Goddard Institute for Space Studies Surface Temperature, GISTEMP Team, 2017; Hansen et al., 2016; the National Oceanic and Atmospheric Administration, NOAA, Zhang et al., 2017). The climate between 1760 and 1900 has relatively small long-term trends, characterized by internal variability and punctuated by brief cooling events caused by aerosol loading from several major volcanic eruptions (Hartmann et al., 2013). We define a pre-industrial period in the next sub-section, which allows us to determine the relative global changes between current conditions and the +1.5 and +2.0 °C Worlds.

From a climate perspective it is theoretically not necessary to specify the exact year for the hypothetical +1.5 or +2.0 °C Worlds as we define this period to be in a steady state. However, the selection of a stabilization year is affected by long-term trends in land use, ozone hole recovery, and aerosol concentrations, which alter the carbon and radiation balances needed to stabilize climate conditions (Mitchell et al., 2017). The stabilization target year also has large implications beyond climate conditions themselves, owing to transient (time-evolving) pathways for socioeconomic development (O'Neill et al., 2014), greenhouse gas concentration emissions (Moss et al., 2010), climate policy (Kriegler et al., 2014), and technological and policy developments affecting a sector like agriculture (Antle et al., 2015; Ruane et al., 2018). Here we concentrate on stabilized climates rather than the temporal progressions (e.g., peak and overshoot, linear, or asymptotic approaches) that could achieve this state.

Representing the stabilized end climate states for the +1.5 and +2.0 °C Worlds is a challenge given that climate model simulations are typically driven by sets of greenhouse gas emissions and socioeconomic development pathways that result in evolving trajectories of climate changes extending from the present into the future (SRES et al., 2000; Moss et al., 2010; Taylor et al., 2012; Eyring et al., 2016). Given that the Coupled Model Intercomparison Project (CMIP) is currently between its 5th and 6th phases (Taylor et al., 2012; Eyring et al., 2016), investigations of +1.5 and +2.0 °C Worlds require either new simulations performed outside of the CMIP protocols or the extraction of a representative warming signal from existing CMIP5 simulations.

2.1. HAPPI stabilization scenarios of +1.5 and +2.0 °C global warming

The primary source of climate information examined in this study are projections from the Half a degree Additional warming, Projections, Prognosis and Impacts project (HAPPI; Mitchell et al., 2017). HAPPI is designed to compare current climate (defined as the 2006–2015 period) with stabilization scenarios for the +1.5 and +2.0 °C Worlds (nominally run for the 2106–2115 period). HAPPI's rapid mobilization of the climate modeling community enables an ensemble of simulations focused on the +1.5 and +2.0 °C Worlds, providing updated models, specified scenarios, and enhanced focus on extreme events in these projections of relatively low global temperature changes. Key attributes of the HAPPI Tier 1 experiments are presented in Table 1, with further information in -the supplementary material and enhanced detail provided by Mitchell et al. (2017).

Table 2 shows the GCMs that provided HAPPI experiment output analyzed in this study according to three analysis approaches. First, *aggregate* statistics were calculated to represent the full GCM ensemble's changes in monthly mean maximum and minimum temperatures, total precipitation, the number of rainy days, and the standard deviation of daily maximum and minimum temperatures for each grid cell. These were then re-gridded to a common ½° × ½° grid to drive gridded crop model analyses (Ruane et al., 2018). Second, climate changes based on the aggregate statistics were then imposed on observational data using

Table 1
HAPPI reference and simulation climate periods.

Climate Period	Years	$[CO_2]$[a]	Notes
Pre-Industrial[b]	1861–1880	288 ppm	Pre-industrial period with relatively few volcanic eruptions
Current	2006–2015	390 ppm	Based on CMIP historical simulation (coupled models initiated 100+ years prior; not expected to exactly match observed interannual variability)
+1.5 °C World	2106–2115	423 ppm	Based on CO_2 and sea-surface temperature patterns from end-of-century RCP2.6 simulations.
+2.0 °C World	2106–2115	487 ppm	Based on CO_2 and sea-surface temperature patterns from end-of-century RCP2.6 and RCP4.5 simulations.

[a] Current and pre-industrial $[CO_2]$ determined from RCP scenarios described by Moss et al. (2010).
[b] The Pre-Industrial period was used to determine the +1.5 and +2.0 °C levels but was not directly simulated.

Table 2
Global climate model (GCM) ensemble members included in the AgMIP CGRA study, including initial condition ensembles for multiple models in the a) HAPPI simulations and b) a multi-model ensemble from CMIP5. For further information on HAPPI GCMs see Mitchell et al. (2017), and on CMIP5 GCMs see Ruane et al. (2017) and Flato et al. (2013). *Aggregate* HAPPI outputs are statistical summaries of broader ensemble used for mean impacts, while *daily* outputs included enabled distributional analysis across all ensemble members. Access date reflects output versions.

a) HAPPI GCM ensemble members

Global Climate Model	HAPPI Current	HAPPI + 1.5 °C	HAPPI + 2.0 °C	Horizontal Resolution (Latitude × Longitude)	Access Date
CanAM4 *(aggregate)*	100	100	100	2.81° × 2.81°	06/2017
CAM4-2degree *(aggregate)*	500	500	500	1.88° × 2.5°	06/2017
CAM4-2degree *(daily)*	20	20	20	0.5° × 0.5°	09/2017
HadAM3P *(aggregate)*	94	83	86	1.25° × 1.88	06/2017
MIROC5* *(aggregate)*	160	100	100	1.41° × 1.41°	06/2017
MIROC5* *(daily)*	20	20	20	0.5° × 0.5°	08/2017
NorESM1* *(aggregate)*	125	125	125	0.94° × 1.25°	06/2017
NorESM1* *(daily)*	20	20	20	0.5° × 0.5°	09/2017

b) CMIP5 GCMs from which Historical and RCP4.5 outputs were analyzed (one simulation each).

Global Climate Model	Horizontal Resolution (Latitude × Longitude)	Access Date
ACCESS1-0	1.25° × 1.88°	02/2012
BCC-CSM1-1	2.81° × 2.81°	07/2011
BCC-CSM1-1-m	1.13° × 1.13°	04/2016
BNU-ESM	2.81° × 2.81°	04/2012
CanESM2	2.81° × 2.81°	04/2011
CCSM4	0.94° × 1.25°	11/2011
CESM1-BGC	0.94° × 1.25°	03/2012
CMCC-CM	0.75° × 0.75°	05/2015
CMCC-CMS	1.88° × 1.88°	05/2015
CNRM-CM5	1.41° × 1.41°	05/2015
CSIRO-Mk3-6-0	1.88° × 1.88°	04/2012
EC-Earth	1.13° × 1.13°	04/2016
FGOALS-g2	2.81° × 2.81°	03/2012
GFDL-CM3	2° × 2.5°	07/2013
GFDL-ESM2G	2° × 2.5°	11/2011
GFDL-ESM2M	2° × 2.5°	11/2011
GISS-E2-H	2° × 2.5°	03/2013
GISS-E2-R	2° × 2.5°	05/2012
HadGEM2-AO	1.25° × 1.88°	05/2015
HadGEM2-CC	1.25° × 1.88°	01/2012
HadGEM2-ES	1.25° × 1.88°	01/2011
INMCM4.0	1.5° × 2°	06/2011
IPSL-CM5A-LR	1.88° × 3.75°	06/2011
IPSL-CM5A-MR	1.27° × 2.5°	10/2011
IPSL-CM5B-LR	1.88° × 3.75°	05/2015
MIROC5	1.41° × 1.41°	07/2011
MIROC-ESM	2.81° × 2.81°	10/2011
MPI-ESM-LR	1.88° × 1.88°	08/2011
MPI-ESM-MR	1.88° × 1.88°	10/2011
MRI-CGCM3	1.13° × 1.13°	08/2011
NorESM1-M	1.88° × 2.5°	06/2011

Note: * HAPPI versions of MIROC5 and NorESM1 are updated versions of similar models used for CMIP5.

a quantile-mapping approach to produce bias-corrected future driving conditions (Ruane et al., 2015a, b), which we applied to point-based simulations (Ruane et al., 2018). Third, *daily* outputs were bias-corrected to the same grid using a quantile-mapping method to match observational statistics in order to capture shifts in inter-annual and intra-seasonal extremes while maintaining long-term trends (Hempel et al., 2013; Schleussner et al., 2018). Daily scenarios have been applied to West African analyses (Faye et al., 2018) and a global examination of agricultural extreme events (Schleussner et al., 2018). Further dynamical and statistical downscaling approaches, which could have provided additional detail on shifts in the characteristics of extreme events, were not available for this rapid assessment.

2.2. Application of the 1980–2009 recent observed climatology

Many existing AgMIP model analyses and projection frameworks participating in the AgMIP CGRA use the 1980–2009 period for crop model calibration ('1995 climate'; as provided by the Agricultural Modeling version of the Modern-Era Retrospective Analysis for Research and Applications, AgMERRA; Ruane et al., 2015a). To enable the use of these resources in agricultural assessments of the +1.5 and +2.0 °C Worlds, we extend HAPPI simulations to estimate differences between the 1995 climate and HAPPI simulations of its current climate (2006–2015; '2010 climate') and the +1.5 and +2.0 °C Worlds. HAPPI simulations directly provide the difference between the 2010 climate and the +1.5 and +2.0 °C Worlds. However, representing the remaining difference between the 1995 and 2010 climates is a challenge as we cannot observe a similar 30-year climatology centered on 2010 and HAPPI simulations do not include 1995.

We employ a simple pattern-scaling approach to estimate how a climatological variable Q (e.g., maximum daily temperatures, precipitation, the number of rainy days, the standard deviation of minimum temperatures) changes between 2010 and 1995 at any given longitude (*i*) and latitude (j) from the ½ º x ½ º global grid:

$$\Delta Q_{i,j,[2010-1995]} = \frac{\Delta Q_{i,j,[1.5-2010]}}{\Delta T_{Global,\,[1.5-2010]}} \times \Delta T_{Global,\,[2010-1995]} \quad (1)$$

The ratio in Eq. (1) represents the rate of local change in Q in response to a change in global temperature, a pattern that may then be multiplied by any similar global temperature change. This is generated by calculating the local change in Q between the HAPPI ensemble average +1.5 °C World and current period simulation (2010 climate) and then dividing by the additional global temperature changes expected in the +1.5 °C World simulation (0.58 °C). This scaling factor is then multiplied by the observed warming between 1995 and 2010 ($\Delta T_{Global,[2010\text{-}1995]}$ = 0.25 °C) drawn from the ensemble of historical temperature products (BEST, GISS, HadCRUT4, and NOAA; note that these observations indicate that the 2010 climate is 0.92 °C warmer than pre-industrial conditions). This results in an estimate of the local offset for the 1995–2010 period, with the process repeated for each month. The same offset is used to calculate climate shifts associated with both the +1.5 and +2.0 °C Worlds so that their differences are determined solely by HAPPI simulations. More complex pattern scaling approaches were not feasible given temporal constraints related to stakeholder interest in the +1.5 °C and +2.0 °C Worlds (Tebaldi and Arblaster, 2014). While this approach likely contributed to local biases (Lopez et al., 2014), patterns for HAPPI models were largely consistent when compared against patterns derived from the +2.0 °C World for all but the MIROC5 GCM, which showed polar regions accounting for an increasing proportion of global temperature rise at the expense of other land areas (not shown).

2.3. CMIP5 transient scenarios of +1.5 and +2.0 °C global warming

Alternative representations of the +1.5 and +2.0 °C Worlds are derived from CMIP5 transient simulations whereby climate evolves from anthropogenic and natural influences over the historical period (1850–2005) and future decades (RCPs covering 2006–2100; Moss et al., 2010). As our interest is in understanding the challenges today's agricultural sector will face from future climate change, we utilize the recent observable 1980–2009 climatology (1995 climate) used in many AgMIP analyses for each GCM (drawing from RCP4.5 for 2006–2009). Note that this period had already warmed 0.67 °C above the 1861-1880 pre-industrial period according to the observational products ensemble. For each GCM, +1.5 and +2.0 °C Worlds are thus defined by their transient thresholds, or the period in which global mean surface temperatures in the transient simulation reach 0.83 °C and 1.33 °C, respectively, above this 1995 climate.

We calculate corresponding threshold years for each GCM and RCP, then construct a centered 30-year average climatology (to elevate the mean climate changes above internal variability; WMO, 1989) for comparison to the current period. Threshold years differ by GCM (depending on transient climate sensitivity) and among RCPs, with earlier thresholds reflecting higher climate sensitivity in some GCMs or the accelerated accumulation of greenhouse gases in RCP8.5 compared to RCP2.6. As many of the RCP2.6 simulations do not reach the +2.0 °C threshold, we focus on the ensemble response of 31 RCP4.5 GCMs in Table 2 given that GCM differences in regional patterns of temperature and precipitation change tend to be robust across RCP and time horizon in the 21st century (Ruane and McDermid, 2017).

Differences in climate change projections between the transient threshold and the same GCM at stabilization merit further study, with differences relating to aerosol and land-use patterns within the transient RCPs as well as a lag between radiative imbalances and equilibration within the climate system. For this study we assume that this effect is small compared to differences between the GCMs captured in the CMIP5 ensemble. Model versions (among models that contributed to both CMIP5 and HAPPI) likely also contribute to differences between transient and stabilization scenarios, as HAPPI simulations (which were conducted largely in 2016 and 2017) used updated versions compared to CMIP5 simulations completed before 2013.

Rising CO_2 concentrations are the largest radiative forcing factor contributing to anthropogenic climate change (IPCC, 2013). The direct impact of CO_2 on photosynthesis merits additional focus for agricultural impacts (Boote et al., 2010; O'Leary et al., 2015; Kimball, 2016; Deryng et al., 2016). CO_2 concentrations in the CMIP5 transients were above HAPPI's recommended 423 ppm at the +1.5 °C crossing point, but below HAPPI's 487 ppm at the +2.0 °C crossing point (Fig. S1). These results suggest that the change in CO_2 concentration and its impacts on agricultural systems are likely overestimated in HAPPI-driven +2.0 °C analyses. Radiative disequilibrium at transient crossing points also likely overestimates stabilization CO_2 concentrations. For example, van Vuuren et al. (2015) indicated that CO_2 concentrations must be kept below 450 ppm to have a 67% probability of keeping global temperature rise below +2.0 °C.

2.4. Regional growing seasons

HAPPI and CMIP5 transient projections were distributed onto a ½° x ½° grid using a nearest-neighbor approach in order to facilitate ensemble statistics and agro-climatic analyses. Growing seasons (Julian day ranges) for each grid cell were drawn from the AgMIP Global Gridded Crop Model Intercomparison and were assumed to remain constant in current and future worlds (Elliott et al., 2015). Each grid cell's growing season aims to represent the practice of the majority of farming systems even though many regions include a wide diversity in sowing dates. Static (~2005) cropped areas from the Spatial Production Allocation Model database (SPAM) provide the basis for weighted spatial averages of agro-climatic changes associated with the +1.5 and +2.0 °C Worlds (You et al., 2014). They also form the basis of agricultural area masks to focus figures on grid cells with > 10 ha rainfed crop area.

Here we highlight rainfed seasons as they are vulnerable to both temperature and precipitation change impacts. Irrigated systems will face similar temperature challenges but are largely unaffected by precipitation changes other than through supply of managed water resources. Wheat growing seasons include both spring and winter wheat systems – in regions where both are grown we examine only the system with higher mean production in the AgMIP Global Gridded Crop Model Intercomparison (GGCMI) historical period simulations (Müller et al., 2017). For winter wheat we examine climate changes during the final 90 days before average maturity to avoid the dormant vernalization period that follows early planting. Wheat tends to be grown earlier in the season than maize, rice, and soy, which are most often grown in the local spring and summer (Fig. S2).

Comparison of climate shifts during the local growing season (ΔT_{GS} and ΔP_{GS}) against the annual climate changes (ΔT_{Ann} and ΔP_{Ann}) helps us identify regions where agricultural challenges are projected to be different than the annual signal suggests. We first look for large magnitudes of difference across multiple models, classifying local growing season changes as 'substantially warmer than annual changes' or 'substantially cooler than annual changes' if $\Delta T_{GS} - \Delta T_{Ann} > 0.2$ °C or $\Delta T_{GS} - \Delta T_{Ann} < -0.2$ °C (respectively) for 3 of the 5 HAPPI models. We next examine areas that do not meet those criteria for consistency in the direction of the difference, classifying local growing season changes as 'consistently warmer than annual changes' if $\Delta T_{GS} - \Delta T_{Ann} > 0$ °C for all HAPPI models. We do the same in the opposite direction for 'cooler' classifications, and then all remaining grid cells are designated as 'small or inconsistent changes'. A similar procedure classified 'wetter' and 'drier' local growing seasons using a threshold of +/-5% difference (compared to current period climate) for substantially different ΔP_{GS}. Note that areas meeting both the 'substantially' and 'consistently' different criteria are classified as 'substantially' different.

3. Results of climate change projections for agricultural regions

The +1.5 and +2.0 °C Worlds are defined by their global mean temperature increases, yet projections reveal important variations across regions, seasons, and the characteristics of climate extremes.

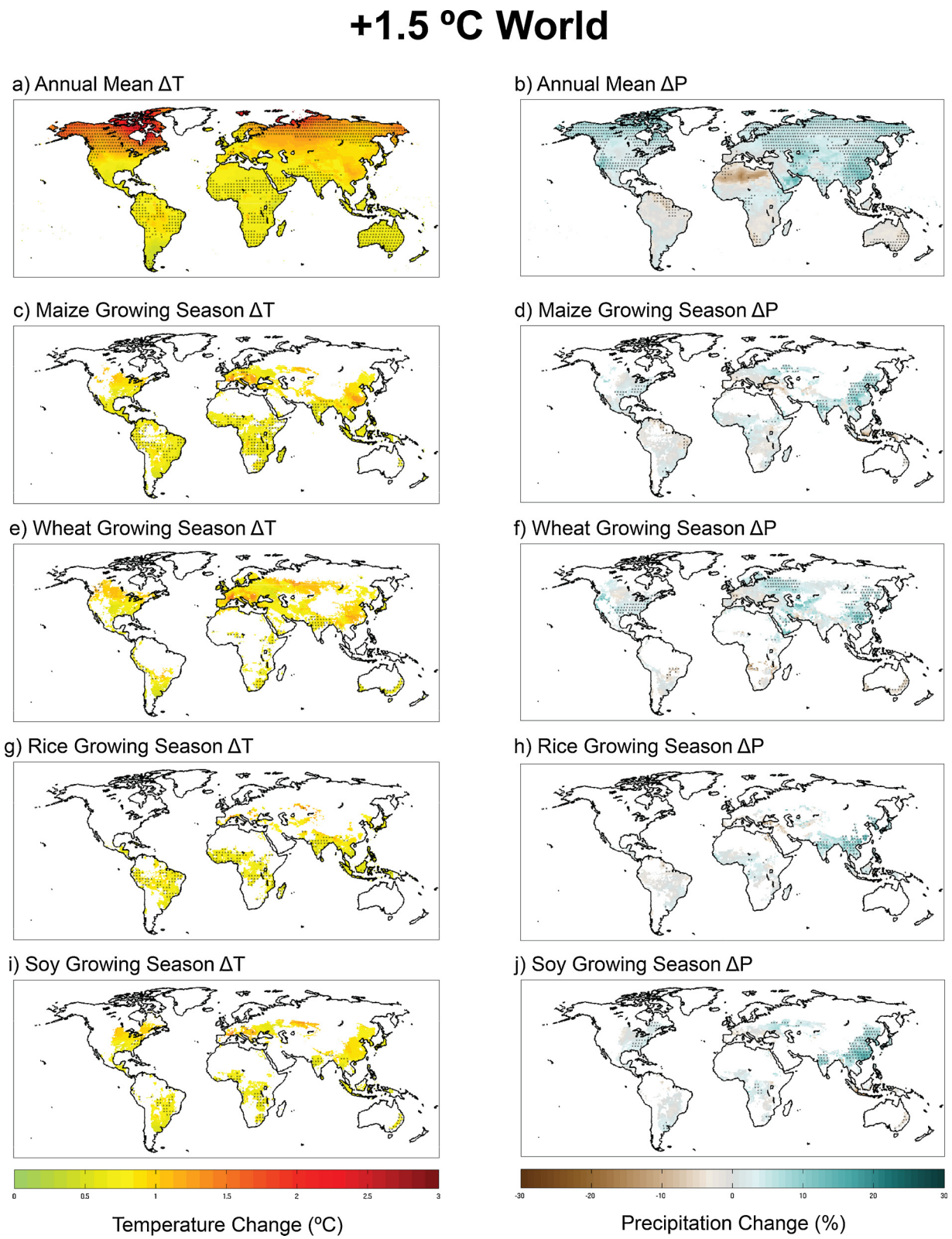

Fig. 1. +1.5 °C World (a,c,e,g,i) temperature and (b,d,f,h,j) precipitation changes compared to current climate for (a,b) all land areas and seasons; (c,d) rainfed maize; (e,f) rainfed wheat; (g,h) rainfed rice; (i,j) rainfed soy. These maps are the basis for estimating local climate change patterns between the 1995 Climate used by AgMIP protocols and the 2010 climate used by HAPPI. Hatch marks for temperature indicate that median changes are greater than twice the range among GCMs, and hatch marks for precipitation indicate agreement on the direction of change by 4 of the 5 HAPPI models. Grid cells with < 10 ha rainfed crop area in the SPAM dataset (You et al., 2014) are omitted to focus on regions with substantial production.

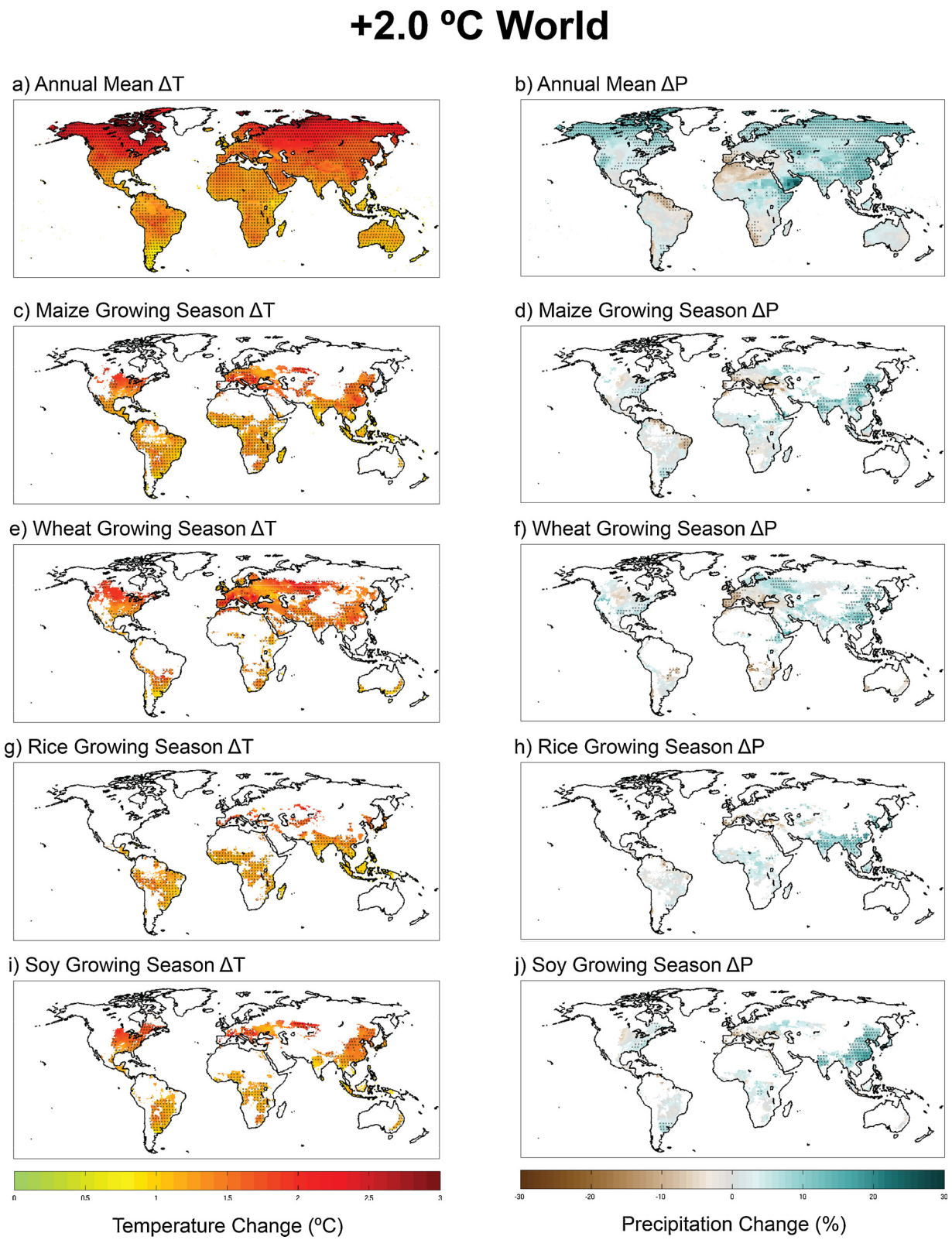

Fig. 2. +2.0 °C World (a,c,e,g,i) temperature and (b,d,f,h,j) precipitation changes compared to current climate for (a,b) all land areas and seasons; (c,d) rainfed maize; (e,f) rainfed wheat; (g,h) rainfed rice; (i,j) rainfed soy. Hatch marks and area mask as in Fig. 1.

Uncertainty is heightened for phenomena simulated at finer temporal and spatial scales where there is greater influence from physical processes beyond the limit of climate model resolution and a lack of aggregation. Assessments of agricultural risks are reliant on this fine-scale information given the potential for non-linear climatic responses and the application of crop models on a hectare scale in AgMIP (Asseng et al., 2013, 2015; Bassu et al., 2014; Ruane et al., 2014; Li et al., 2015; Pirttioja et al., 2015; Fleisher et al., 2017). Simulations for the CGRA assessment of +1.5 and +2.0 °C Worlds likewise need information with more detail than the global annual mean temperature analysis,

particularly given that the ½º x ½º resolution grids utilized for global crop model simulations are finer than the horizontal resolution of most global climate models (Ruane et al., 2018; Rosenzweig et al., 2018).

3.1. Mean changes for +1.5 and +2.0 °C worlds

Mean annual climate changes in HAPPI projections of the +1.5 and +2.0 °C Worlds compared to the 2010 current climate (Figs. 1a–b and 2a–b, respectively) generally reflect the major patterns described in recent IPCC assessments, with the signal of change becoming more clear as global mean temperature increases (Collins et al., 2013). These simulations highlight uncertainties in HAPPI models related to the distribution of additional energy trapped in the system by greenhouse gases and other anthropogenic influences, differentiating climate challenges for agricultural regions. Rosenzweig et al. (2018) provide a comprehensive example of HAPPI uncertainty in displaying each GCM projection for rainfed maize climate changes.

Warming over land generally exceeds the global mean temperature rise since 2010 (~0.58 °C and ~1.08 °C for the +1.5 and +2.0 °C Worlds, respectively; recall that 2010 was 0.92 °C above pre-industrial) owing to the ocean's larger aggregate heat capacity. The poles also warm faster than the tropics given snow-ice albedo feedbacks and the prominence of high-latitude longwave radiation emissions in the global energy balance. Arid region temperatures rise more rapidly as a lack of available soil moisture limits evaporation and causes a larger portion of excess energy to go into sensible heat. Farmlands are not evenly distributed around the globe, however; agricultural regions are generally rare in arid regions and at higher latitudes where sub-freezing temperatures shorten the viable growing season. Agricultural area-weighted temperature changes are therefore closer to the global average but depend on a given GCM's distribution of the warming signal owing to ocean-atmosphere heat exchanges, radiative feedback processes, and atmospheric circulation patterns. Projections of the +1.5 °C World show stronger agreement in temperature changes at low and high latitudes as overall temperature changes are comparable to the range between GCM projections; however, many of the mid-latitude agricultural regions have substantial GCM spread. In the +2.0 °C World, projected temperature changes are at least double the GCM range for most areas and seasons. Uncertainty is larger over prominent wheat-growing regions of Eastern Europe and central North America in addition to regions where agriculture is less prominent, such as over the Tibetan Plateau, the inner Amazon, and north of the Caspian Sea.

In many regions and agricultural seasons there is not strong agreement in the direction of precipitation changes (Fig. 1b). Mean annual precipitation generally increases over land given an overall increase in evaporation and transpiration as warmer conditions lead to higher vapor pressure deficits even when relative humidities are maintained. Regional differences reflect a more vigorous water cycle that exacerbates given atmospheric moisture convergence patterns wherein convergence (wet) areas generally become wetter and divergence (dry) areas are more prone to drying (Trenberth, 2011; Collins et al., 2013). Notable exceptions include drying over the Amazon (due in part to land cover changes) and an increase in precipitation over Eastern Africa and Western Asia (likely connected to large-scale circulation patterns associated with the South Asian monsoon; Christensen et al., 2013). The South Asian monsoon benefits from more water vapor transport as higher atmospheric specific humidities overwhelm slight reductions in the strength of the monsoon circulation (Christensen et al., 2013). A reduction in aerosols associated with RCP2.6 end-of-century forcings utilized in HAPPI simulations also reduces the inhibition of precipitation in South and Southeast Asia (Carl-Friedrich Schleussner, personal communication).

Changing precipitation patterns and shifts in the hydrologic cycle will drive shifts in soil moisture and evapotranspiration demand, which HAPPI and CMIP earth system models simulate using dynamic vegetation models of varying complexity (most have a relatively simple representation of agricultural systems; McDermid et al., 2017). Projected changes in soil moisture and evapotranspiration are beyond the present study's focus on climate scenarios for agricultural modeling applications given that AgMIP's agricultural models simulate these quantities internally.

3.2. Unique characteristics of changes for growing seasons

Agricultural systems are most vulnerable to climate changes affecting major production regions and core growing seasons. HAPPI projections for the +1.5 and +2.0 °C Worlds feature substantial seasonal variation reflecting the annual cycle of atmospheric circulation patterns, local radiation balances, and shifts in land surface characteristics.

Figs. 1c–j and 2c–j show the growing season temperature and precipitation change patterns over regions with substantial maize, wheat, rice, and soy production. Many of the highest temperature and precipitation change regions are not agriculturally prominent (e.g., high latitudes, high elevations, and arid regions), and thus the overall comparison reveals more muted climate changes for agricultural regions and seasons than for the annual mean global picture. Regional temperature patterns from the annual change map are generally maintained from season to season, indicating that these are larger than monthly differences in temperature change at any given location. Growing season and annual precipitation changes are similar because rainfed cultivation tends to occur in the local rainy season, which has a disproportionate influence on total annual rainfall totals. Process-based models and empirical studies show that global cereal production responds negatively to increasing temperatures (Rosenzweig et al., 2014; Asseng et al., 2013; Bassu et al., 2014; Challinor et al., 2014; Li et al., 2015; Zhao et al., 2017), and the food system implications of these projections are explored further within the AgMIP CGRA (Ruane et al., 2018; Rosenzweig et al., 2018).

Zonal patterns are readily apparent in growing season climate change characteristics using the classifications of 'substantially' and 'consistently' different than annual climate changes presented in Fig. 3 for each growing season in the +1.5 °C World (Fig. S3 displays the corresponding +2.0 °C World maps). Growing seasons are generally projected to warm at a slower rate than the annual mean in the humid tropics (e.g., in Brazil, Central and Western Africa, Southern India, and Southeast Asia). In these regions cultivation is aligned with a strongly seasonal rain band or wet monsoon phase that reduces local warming compared to the dry seasons. Growing seasons in the semi-arid tropics (e.g., Mexico, East Africa, and northern India) tend to warm consistently faster than the annual signal, and in Mediterranean climates (including Eastern Australia) ΔT_{GS} is accelerated in association with drying trends. ΔT_{GS} for high-latitude agricultural regions is lower than the annual average given the pronounced snow-ice feedbacks that dominate the non-agricultural winter season. The region around Uruguay is an exception to this zonal pattern, with heightened ΔT_{GS} potentially linked to a precipitation pattern that also enhances seasonal rainfall.

ΔP_{GS} is substantially and consistently wetter than ΔP_{Ann} over the South Asian and Southeast Asian monsoon, with exceptions where the local growing season does not correspond with the main monsoon rains (e.g., Indonesian maize, Indian wheat; see Fig. S3). Mediterranean drying affects agricultural seasons more strongly than the annual average as it is most acute during the agricultural spring and summer seasons (see also Collins et al., 2013). A dipole over North America indicates enhanced growing season drying in the continental interior and wetter conditions in the Southern and Eastern United States, exacerbating the annual trend. ΔP_{GS} is drier than ΔP_{Ann} for most Southern Hemisphere wheat growing seasons, suggesting the potential for shifts in planting and harvest dates as seasonal patterns change amidst a generally drying trend in Australia, Southern Africa, and portions of South America.

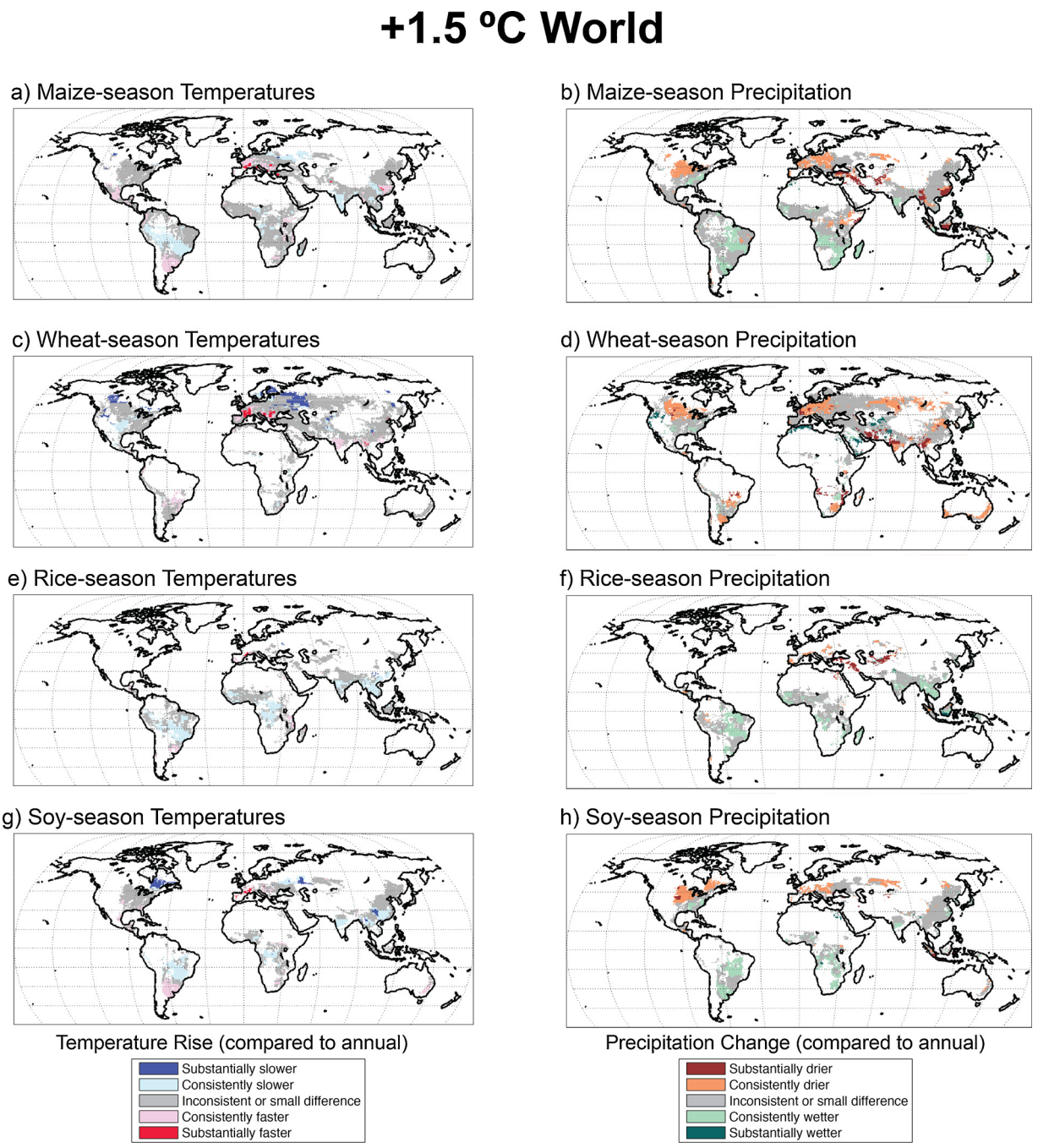

Fig. 3. Classes of +1.5 °C World local (a,c,e,g) temperature and (b,d,f,h) precipitation change deviations for growing seasons compared to annual changes for (a,b) rainfed maize; (c,d) rainfed wheat; (e,f) rainfed rice; (g,h) rainfed soy. 'Substantially' different indicates that growing season change differences in at least 3 out of the 5 HAPPI models changed at a pace that was 'faster' or 'slower' than 0.2 °C for temperatures or 5% for precipitation ('drier' or 'wetter') compared to the annual mean, while 'Consistently' different indicates that all 5 HAPPI GCMs agreed on the sign of difference. Areas that meet both the 'substantially' and 'consistently' criteria are designated as 'substantially' different. Area mask as in Fig. 1. Note that Fig. S3 presents corresponding results for the +2.0 °C World.

Regional patterns in temperature and precipitation changes are largely consistent between the +1.5 and +2.0 °C Worlds. The magnitude of these regional changes is broadly consistent with an approximate doubling in deviation from today's conditions between the 1.5 and 2.0 °C Worlds (tracking the global mean temperature rises of 0.58 and 1.08 °C, respectively).

3.3. Changes in agro-climatological extremes

The stability of agricultural systems under a +1.5 or +2.0 °C World will depend not only on mean climate conditions but also on interannual variations that exacerbate the risk of poor harvests that stakeholders must manage. Fig. 4 demonstrates the ways in which the distributions of extreme heat and drought years shift in comparison to current climate, utilizing the subset of HAPPI daily bias-corrected and downscaled data (each with 200 seasons from 20 ensemble-members' 10-year simulations). In most tropical and extra-tropical regions, rainfed maize season temperatures in the +1.5 °C World exceed the current period 'extreme heat' year (defined as the 90th percentile growing season mean temperature) in more than half of all years (Fig. 4a). This is true even in Southeast Asia where mean temperatures rise more slowly, as the extreme temperature threshold is low owing to

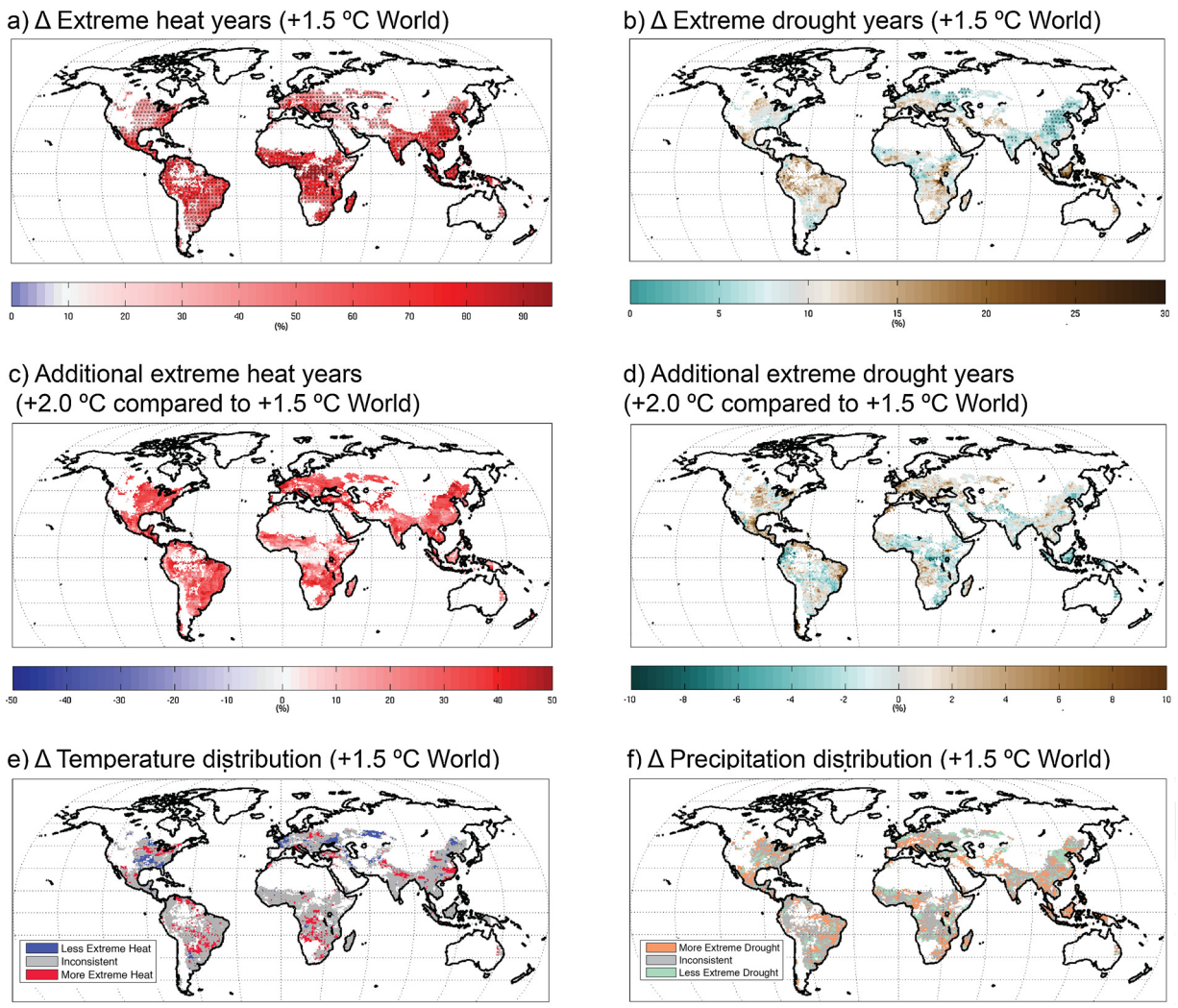
a) Δ Extreme heat years (+1.5 ºC World)
0 10 20 30 40 50 60 70 80 90
(%)
b) Δ Extreme drought years (+1.5 ºC World)
0 5 10 15 20 25 30
(%)
c) Additional extreme heat years
(+2.0 ºC compared to +1.5 ºC World)
-50 -40 -30 -20 -10 0 10 20 30 40 50
(%)
d) Additional extreme drought years
(+2.0 ºC compared to +1.5 ºC World)
-10 -8 -6 -4 -2 0 2 4 6 8 10
(%)
e) Δ Temperature distribution (+1.5 ºC World)
Less Extreme Heat
Inconsistent
More Extreme Heat
f) Δ Precipitation distribution (+1.5 ºC World)
More Extreme Drought
Inconsistent
Less Extreme Drought

Fig. 4. Shifts in extreme conditions for rainfed maize season in +1.5 °C World compared to current climate. (a) Change in the frequency of extreme heat years (above 90th percentile in current climate); (b) change in the frequency of extreme drought years (below 10th percentile in current climate); (c) additional extreme heat years in the +2.0 °C World compared to the +1.5 °C World; (d) additional extreme drought years in the +2.0 °C World compared to the 1.5 °C World; (e) change in the skewness of seasonal temperature distribution; (f) change in the skewness of seasonal precipitation distribution. Hatch marks in (a) and (b) indicate reduction in frequency of more than ¼ or increases of more than ½. Regions marked as inconsistent in (e,f) unless 2 of the 3 HAPPI daily °GCMs demonstrate substantial shifts in skewness (percentile change differences greater than 0.1 °C for temperature and 2% for precipitation). Area mask as in Fig. 1c and d.

limited interannual variability in the current climate. A dramatic increase in extreme years is also projected in mid-latitude regions including portions of Northeast Asia, Southern Europe, and the Eastern United States. Thus, even relatively low levels of warming can lead to substantial anomalies, and these are particularly noticeable where current interannual variation is low even as mean climate changes are lower than those at higher latitudes (Fig. 1c).

Diffenbaugh et al. (2018) likewise noted dramatic increases in extreme conditions under +1.5 and +2.0 °C warming scenarios. Changes in mean conditions alone can increase the probability of crop failures as growing season climate moves closer to dangerous biophysical thresholds (Hatfield et al., 2011; Lobell et al., 2011, 2013; Zhao et al., 2017). The frequency of 'extreme drought' years in the +1.5 °C World (defined as the 10th percentile growing season total precipitation) generally become less common (occurring less than 10% of the time) in areas where rainfall is increasing Fig. 1d), but the frequency of drought conditions increases in many places where median rainfall changes were small or negative (e.g., Indonesia, Peru, Mexico, the Northern US Plains, Europe) (Fig. 4b).

The additional half-degree warming between the +1.5 and +2.0 °C Worlds is projected to have substantial impacts on extreme conditions. Many mid-latitude regions see 20–40% more years becoming extreme heat years in the +2.0 °C World (Fig. 4c), with smaller increases in the tropics largely because many of those regions already had a high percentage of extreme heat years in the +1.5 °C World (Fig. 4a). Changes between the frequency of extreme drought between the +1.5 and +2.0 °C Worlds (Fig. 4d) show the general exacerbation of changes in the +1.5 °C World patterns (Fig. 4b). However, many areas show a reduction or even slight reversal of these drought frequency trends as the extreme drought years had already been reduced by mean precipitation increases (e.g., in the monsoon regions of South and Eastern Asia).

It is possible that this increase in climate extremes comes simply from changes in mean conditions, so we additionally examine changes in the temperature and precipitation distributions by comparing changes in the extreme percentiles against median changes for each bias-corrected GCM (Fig. 4d and e). If the 90th percentile of the temperature distribution is warming more rapidly than the median, this indicates a skew toward more extreme heat years. This is apparent for many tropical and Asian monsoon regions. The opposite skewness toward less extreme heat years is projected for more northerly latitudes. The Eastern United States inverts this meridional pattern, with more

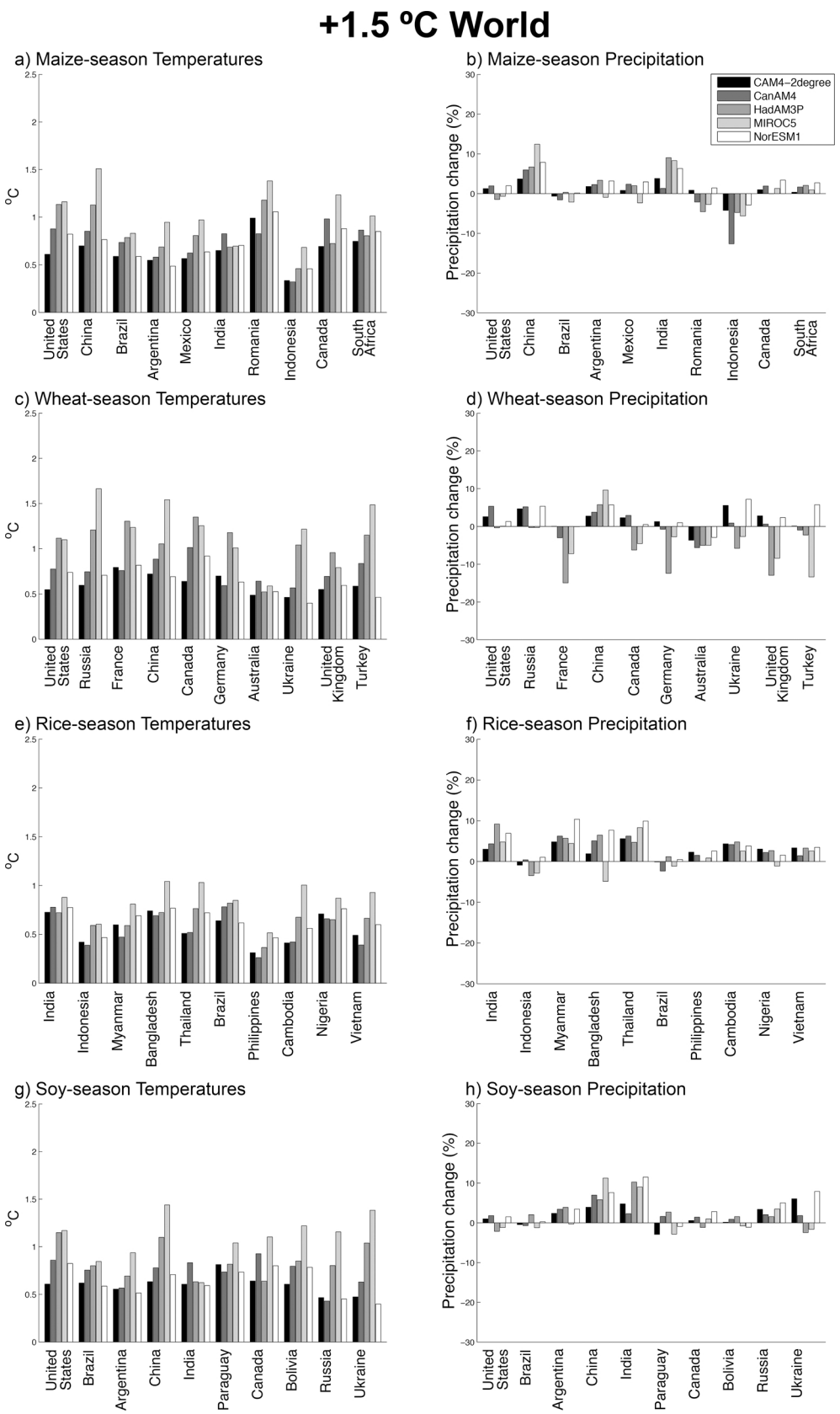

Fig. 5. +1.5 °C World HAPPI projected (a,c,e,g) temperature and (b,d,f,h) precipitation changes compared to current climate, weighted by cropped area within the top 10 producing countries (presented in descending order from left to right) for (a,b) maize; (c,d) wheat; (e,f) rice; (g,h) soy.

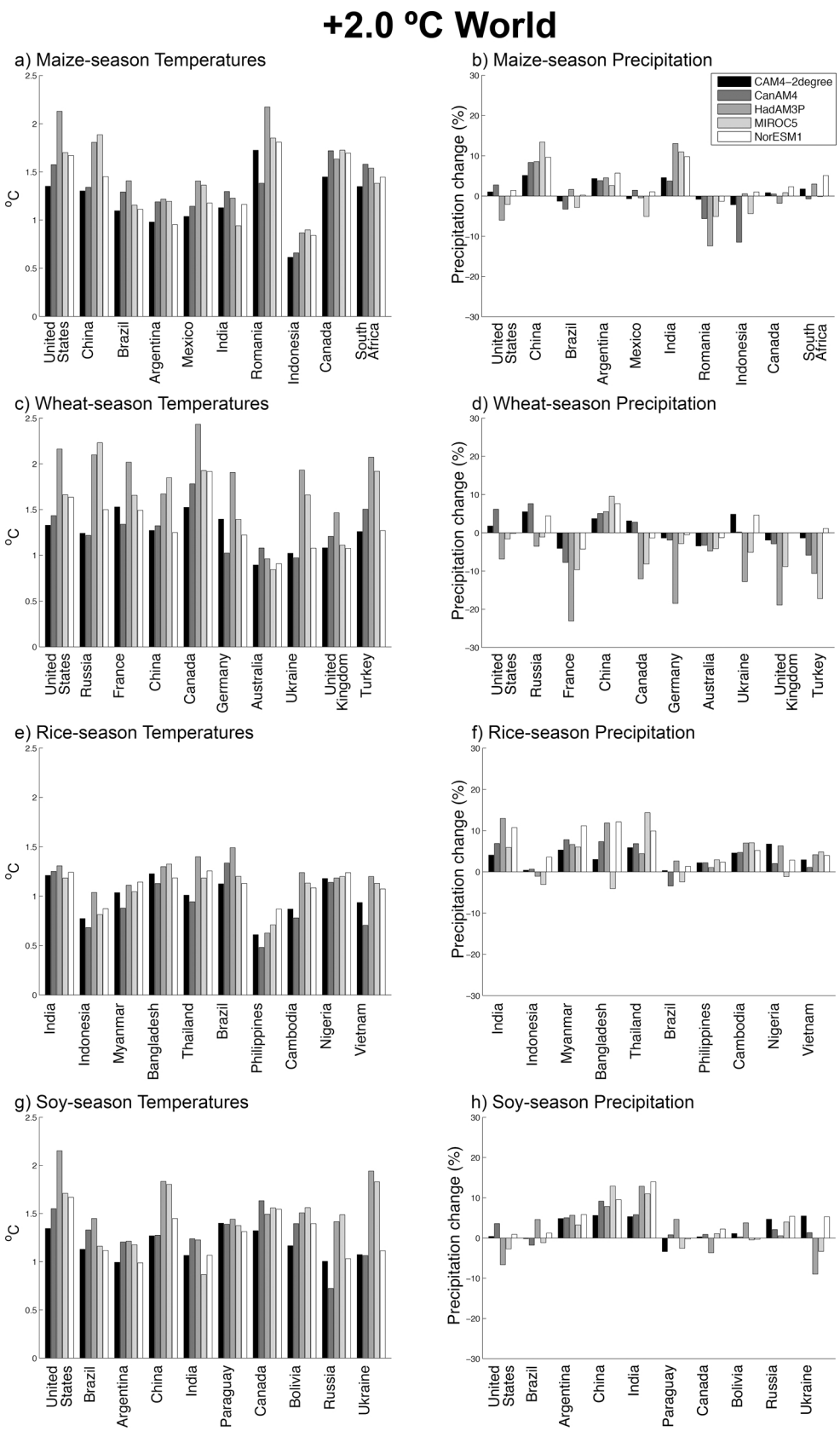

Fig. 6. +2.0 °C World HAPPI projected (a,c,e,g) temperature and (b,d,f,h) precipitation changes compared to current climate, weighted by cropped area within the top 10 producing countries (presented in descending order from left to right) for (a,b) maize; (c,d) wheat; (e,f) rice; (g,h) soy.

extreme heat skewness in the Great Lakes region and less in the Southern US. Skewness toward more or less extreme drought years (whereby the 10th percentile precipitation dries in comparison to the median change) shows much larger spatial variation and no clear large-scale patterns. Schleussner et al. (2018) examine the effects that changing distributions of climate extremes have on yield reliability within the CGRA crop model simulations.

4. Agro-climatic changes for major breadbaskets

Climate change impacts on top cereal-producing countries merit closer investigation as they have a disproportionate influence on global food markets, driving livestock prices in addition to cereal prices given the importance of grain-based animal feed. Climate shocks in these countries may also threaten global food security through disruptions in food exports. As agricultural production is concentrated in breadbaskets within these countries, Figs. 5 and 6 show the mean growing season temperature and precipitation changes (weighted by area growing the rainfed crop within each country) from each HAPPI GCM for the top 10 maize, wheat, rice, and soy production countries for the +1.5 and +2.0 °C Worlds, respectively.

Overall temperatures in these high-producing countries show mean warming that is larger than the inter-GCM spread, providing higher confidence in projections even as warming is lower in the tropics than at higher latitudes. Precipitation changes are mixed, with large variation in sign and magnitude across GCMs and breadbaskets. Wheat growing seasons demonstrate the largest precipitation change variations, while rice seasons are consistent in projecting wetter conditions given the prominence of the Asian monsoons in global rice production (results in Indonesia, Brazil, and Nigeria are less consistent).

Projected changes between the current period and the +1.5 °C World are generally extended in the +2.0 °C World, with similar variation among breadbaskets and GCMs. Although all GCMs have nearly identical global mean surface temperature increases for a given climate stabilization, the patterns of warming (between oceans, land, specific land areas, and different seasons) depend on internal model parameters and structures. MIROC5 stands out as exceptionally warm for many breadbasket regions in the +1.5 °C World, but HadAM3P is most often the warmest over main agricultural countries for the +2.0 °C World. Warming between the +1.5 and +2.0 °C Worlds exceeds the global average 0.5 °C in several breadbaskets (as discussed in Section 3.1), notably including US and Romanian maize, US and Canadian wheat, and US soy. Many leading rice-producing countries are projected to lag the global warming pace given their tropical location and prevailing wetter conditions.

5. Comparing stabilization and transient projections for agricultural model applications

Fig. 7 compares aggregate temperature and precipitation changes over land for HAPPI and CMIP5. Despite being a 5-GCM subset representing a much larger GCM ensemble, the HAPPI simulations display an overall spread that is comparable to that of the 31-member CMIP5 ensemble.

5.1. Annual changes

Annual changes over land in HAPPI and CMIP5 are larger than the global signal, with the land-sea contrast increasing as median land temperatures rise by more than 0.5 °C between the +1.5 and +2.0 °C Worlds (0.59 °C in HAPPI, 0.64 °C in CMIP5). An earlier arrival of +1.5 and +2.0 °C conditions and a higher stabilization ceiling was also noted in projections over the US (Karmalker and Bradley, 2017). As noted in the previous section, MIROC5 produces the largest HAPPI land temperature increases for the +1.5 °C World, but HadAM3P is more extreme for the +2.0 °C World. Precipitation over land increases between the +1.5 °C and +2.0 °C Worlds on average, with increases (0.8% in HAPPI and 0.98% in CMIP5) for that 0.5 °C warming indicating a pace slightly above the 1% K^{-1} noted for global precipitation changes in the CMIP5 ensemble due to an overall amplification of the water cycle and moisture transport (Pendergrass and Hartmann, 2014).

5.2. Growing season changes

ΔT_{GS} for each season (weighted by harvested rainfed area across all land) is more uncertain than the all-land and all-season ΔT_{Ann} across both the stabilization and transient scenarios, as would be expected for more specific geographic regions and seasons. ΔT_{GS} is also lower than ΔT_{Ann} as agricultural lands are disproportionately located away from arid and polar regions that warm most rapidly, in addition to cultivation occurring in the wetter and frost-free months of the year. Much of the accelerated ΔT_{Ann} over land comes from high-latitude regions, so agricultural lands fall increasingly behind the pace of land ΔT_{Ann} in the +2.0 °C World. The largest ΔT_{GS} and ΔP_{GS} uncertainties are in the wheat season, potentially owing to the location of wheat systems predominantly in mid-latitude regions affected by variable storm tracks (recall Fig. 1e). ΔP_{GS} in both HAPPI and CMIP5 ensembles lag behind the ΔP_{Ann} for wheat (owing largely to drier conditions in Europe and central North America), while the rice season has the most dramatic lag in warming and an accelerated increase in precipitation (likely due to the importance of monsoon precipitation changes in the global land signal).

The projected rice-growing season features the largest differences between the HAPPI stabilization and the CMIP5 transient ensembles. Global rice production is dominated by intense rice cultivation in the monsoon regions of Asia that currently experience some of the highest aerosol concentrations in the world. The HAPPI simulations include a dramatic reduction in aerosols according to end-of-century RCP2.6 conditions, while these levels are not achieved in CMIP5 RCP4.5 transients (nor would the same levels be seen in RCP2.6 transients that first reach +1.5 or +2.0 °C warming well before the end of the century). With reduced aerosols the HAPPI simulations warm rice production regions more rapidly, raising global aggregated median rice-season temperatures by 0.19 °C compared to CMIP5 for both stabilization worlds. The signal of aerosols is less clear in rice season precipitation, as there remains substantial uncertainty in GCM simulation of aerosol effects on evaporation, heat pumping, and precipitation inhibition (Ramanathan et al., 2005; Lau and Kim, 2006; Rind et al., 2009; Boucher et al., 2013).

6. Discussion

Mean growing season climate changes and shifts in the distribution of interannual events characterize agricultural system challenges for the +1.5 and +2.0 °C Worlds, although climate changes associated with the +1.5 and +2.0 °C Worlds are small in comparison to end-of-century shifts in transient RCP8.5 simulations (~4–6 °C above pre-industrial conditions from ensemble of 39 GCMs in Collins et al., 2013; Rosenzweig et al., 2014). However, projected conditions in major agricultural regions are likely to require substantial adaptation even under these highly-mitigated climate stabilizations. While cereal-producing regions generally experience a slower pace of warming in growing seasons than other land areas, projected precipitation changes demonstrate high uncertainty and spatial variability that will lead to regional wetting and drying trends even as global precipitation increases slightly. Precipitation patterns over North America indicate that the dipole of a drying continental interior and wetter East and Southeast will be more pronounced in the summertime growing seasons than in the annual average.

Even with these relatively low levels of mean warming farmers are projected to experience a dramatic increase in the probability of what are currently considered extremely hot growing seasons, and many

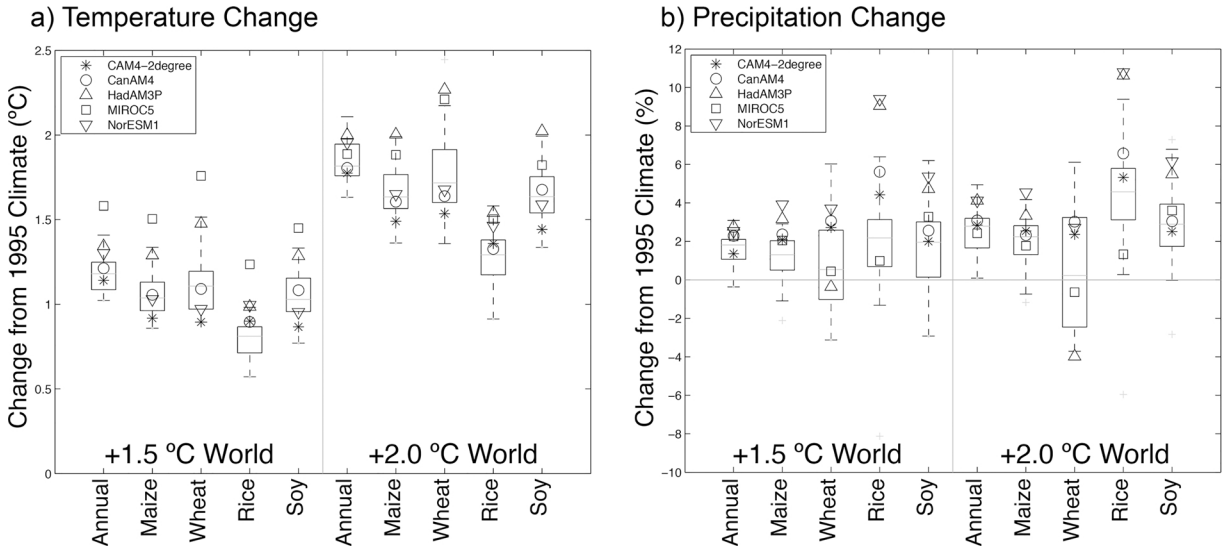

Fig. 7. HAPPI and CMIP5 RCP4.5 (a) temperature changes and (b) precipitation changes compared to current climate for annual conditions across all land areas as well as maize, wheat, rice, and soy seasons weighted according to cropped area. Symbols represent HAPPI simulations, while box-and-whisker diagrams indicate CMIP5 median projections and their interquartile range, while whiskers extend to the last point within an additional 1.5 times the interquartile range.

regions experiencing drier average conditions would also experience an increase in extreme drought seasons. These challenges are apparent even in the +1.5 °C World, and are exacerbated in the +2.0 °C World, particularly as regional warming patterns cause many agricultural regions to warm by more than 0.5 °C between Worlds. HAPPI simulations provide useful insight into these targeted end states, but uncertainties remain owing partially to difficulties in representing desired climate stabilizations rather than simulating transient scenarios. Major production regions for maize, wheat, and soy face larger average temperature increases than rice production regions, which also are more likely to see increases in precipitation although both rice effects may be influenced by HAPPI assumptions about reduced aerosol loading and aerosol effects on Asian monsoon regions. For agricultural applications, CO_2 levels in the +1.5 and +2.0 °C Worlds (and their impact on agricultural systems) remain a major uncertainty that can reverse the overall direction of production changes (Ruane et al., 2018; Rosenzweig et al., 2018).

Agricultural sector impacts for the +1.5 and +2.0 °C Worlds may be characterized by linking the climate conditions described here with biophysical models (to determine climate impacts on plant processes and production), and economic models (to understand profit, trade, and resource allocation). Interdependence of global and regional stakeholders can be explored through markets, policies, global climate, and resource competition. AgMIP Coordinated Global and Regional Assessments utilize the climate scenarios described in Section 2 to represent +1.5 and +2.0 °C World climates for a prototype integrated, multi-disciplinary, multi-scale, and multi-model assessment that explores direct biophysical impacts and their implications for regional and global markets (Ruane et al., 2018; Rosenzweig et al., 2018).

Several important climate-related mechanisms are not directly evaluated here and are needed to further inform the development of effective adaptation strategies for agriculture. Priority areas for scenario generation and future evaluations include:

- Damages from floods and water-logging in farming regions where precipitation is projected to increase (Ruane et al., 2013);
- CO_2 fertilization effects on crops and their interactions with drought (Boote et al., 2010; O'Leary et al., 2015; Kimball, 2016; Deryng et al., 2016);
- Effects of sea-level rise and shifting hurricane intensities on agricultural production in coastal floodplains (Church et al., 2013);
- Acute damages from short-duration heat waves affecting critical crop development stages (Asseng et al., 2015; Maiorano et al., 2017);
- Changes in sowing and harvest dates in response to changing climatic conditions (Tadross et al., 2009; Crespo et al., 2011; Glotter and Elliott, 2016);
- Shifts in major modes of climate variability (e.g., the El Niño/Southern Oscillation or North Atlantic Oscillation; Iizumi et al., 2014);
- Competition over managed water resources (Elliott et al., 2014);
- Shifts in cropping areas associated with climate and socioeconomic development (Wiebe et al., 2015); and
- Crop losses from damaging pests, diseases, and weeds (Savary et al., 2012; Donatelli et al., 2017).

A primary limitation remains the collection and dissemination of high-quality experimental and observational data along the climate-crop-economic-human outcome pathway. Through AgMIP, the agricultural research community is developing improved models and systematic protocols to address many of these gaps.

The combination of HAPPI and CMIP5 projections analyzed here indicate climate challenges for agricultural regions even under high mitigation scenarios. Results and agricultural model impact assessments, particularly those that compare against lower mitigation scenarios with more dramatic climate changes, can inform cost-benefit analysis that weigh the relative burden placed on adaptation, mitigation, and disruption to the agricultural system. By projecting the challenges facing future farmers, we also aim to provide climate condition targets for agricultural technologies that will increase resilience for vulnerable farm systems around the world.

Acknowledgements

The authors thank the HAPPI team (Dann Mitchell, Myles Allen, Carl-Friedrich Schleussner, Peter Uhe, Mamunur Rashid) for calculating aggregate statistics and providing daily bias-corrected and downscaled outputs. We acknowledge the World Climate Research Programme's Working Group on Coupled Modelling, which is responsible for CMIP, and we thank the climate modeling groups (noted in Table 2) for producing and making available their model output. For CMIP the U. S. Department of Energy's Program for Climate Model Diagnosis and Intercomparison provides coordinating support and led development of software infrastructure in partnership with the Global Organization for

Earth System Science Portals. This work was supported by the National Aeronautics and Space Agency Science Mission Directorate (WBS 281945.02.03.06.79) and the US Department of Agriculture (USDA OCE grant 58-0111-16-010). We also thank Greg Reppucci for assistance in preparing figure graphics. Results reflect the findings of the authors and do not necessarily represent the views of the sponsoring agencies.

Appendix A. Supplementary data

Supplementary material related to this article can be found, in the online version, at doi:https://doi.org/10.1016/j.agrformet.2018.05.013.

References

Antle, J.M., Valdivia, R.O., Boote, K.J., Janssen, S., Jones, J.W., Porter, C.H., Rosenzweig, C., Ruane, A.C., Thorburn, P.J., 2015. AgMIP's trans-disciplinary agricultural systems approach to regional integrated assessment of climate impact, vulnerability and adaptation. In: Rosenzweig, C., Hillel, D. (Eds.), The Handbook of Climate Change and Agroecosystems: The Agricultural Model Intercomparison and Improvement Project Integrated Crop and Economic Assessments, Part 1. Imperial College Press, London, pp. 27–44. http://dx.doi.org/10.1142/9781783265640_0002.

Asseng, S., Ewert, F., Rosenzweig, C., Jones, J.W., Hatfield, J.L., Ruane, A.C., Boote, K.J., Thorburn, P., Rötter, R.P., Cammarano, D., Brisson, N., Basso, B., Martre, P., Aggarwal, P.K., Angulo, C., Bertuzzi, P., Biernath, C., Challinor, A.J., Doltra, J., Gayler, S., Goldberg, R., Grant, R., Heng, L., Hooker, J., Hunt, L.A., Ingwersen, J., Izaurralde, R.C., Kersebaum, K.C., Müller, C., Naresh Kumar, S., Nendel, C., O'Leary, G., Olesen, J.E., Osborne, T.M., Palosuo, T., Priesack, E., Ripoche, D., Semenov, M.A., Shcherbak, I., Steduto, P., Stöckle, C., Stratonovitch, P., Streck, T., Supit, I., Tao, F., Travasso, M., Waha, K., Wallach, D., White, J.W., Williams, J.R., Wolf, J., 2013. Uncertainty in simulating wheat yields under climate change. Nat. Clim. Change 3, 827–832. http://dx.doi.org/10.1038/NCLIMATE1916.

Asseng, S., et al., 2015. Rising temperatures reduce global wheat production. Nat. Clim. Change 5 (2), 143–147. http://dx.doi.org/10.1038/nclimate2470.

Bassu, S., Brisson, N., Durand, J.-L., Boote, K., Lizaso, J., Jones, J.W., Rosenzweig, C., Ruane, A.C., Adam, M., Baron, C., Basso, B., Biernath, C., Boogaard, H., Conijn, S., Corbeels, M., Deryng, D., De Sanctis, G., Gayler, S., Grassini, P., Hatfield, J., Hoek, S., Izaurralde, C., Jongschaap, R., Kemanian, A.R., Kersebaum, K.C., Kim, S.H., Kumar, N.S., Makowski, D., Müller, C., Nendel, C., Priesack, E., Pravia, M.V., Sau, F., Shcherbak, I., Tao, F., Teixeira, E., Timlin, D., Waha, K., 2014. How do various maize crop models vary in their responses to climate change factors? Glob. Change Biol. 20 (7), 2301–2320. http://dx.doi.org/10.1111/gcb.12520.

Beddington, J., Asaduzzaman, M., Clark, M., Fernández, A., Guillou, M., Jahn, M., Erda, L., Mamo, T., Van Bo, N., Nobre, C.A., Scholes, R., Sharma, R., Wakhungu, J., 2012. Achieving Food Security in the Face of Climate Change: Final Report from the Commission on Sustainable Agriculture and Climate Change. CGIAR Research Program on Climate Change. Available online at:. Agriculture and Food Security (CCAFS), Copenhagen, Denmark. www.ccafs.cgiar.org/commission.

Boote, K.J., Allen Jr., L.H., Prasad, P.V.V., Jones, J.W., 2010. Testing effects of climate change in crop models. In: Rosenzweig, C., Hillel, D. (Eds.), The Handbook of Climate Change and Agroecosystems. Imperial College Press, Singapore, pp. 109–129.

Boucher, O., Randall, D., Artaxo, P., Bretherton, C., Feingold, G., Forster, P., Kerminen, V.-M., Kondo, Y., Liao, H., Lohmann, U., Rasch, P., Satheesh, S.K., Sherwood, S., Stevens, B., Zhang, X.Y., 2013. In: Stocker, T.F., Qin, D., Plattner, G.-K., Tignor, M., Allen, S.K., Boschung, J., Nauels, A., Xia, Y., Bex, V., Midgley, P.M. (Eds.), Clouds and Aerosols. In: Climate Change 2013: The Physical Science Basis. Contribution of Working Group I to the Fifth Assessment Report of the Intergovernmental Panel on Climate Change. Cambridge University Press, Cambridge, United Kingdom and New York, NY, USA.

Brown, M.E., Antle, J.M., Backlund, P., Carr, E.R., Easterling, W.E., Walsh, M.K., Ammann, C., Attavanich, W., Barrett, C.B., Bellemare, M.F., Dancheck, V., Funk, C., Grace, K., Ingram, J.S.I., Jiang, H., Maletta, H., Mata, T., Murray, A., Ngugi, M., Ojima, D., O'Neill, B., Tebaldi, C., 2015. Climate Change, Global Food Security, and the U.S. Food System. 146 pages. Available online at. . doi: 10.7930/J0862DC7. http://www.usda.gov/oce/climate_change/FoodSecurity2015Assessment/FullAssessment.pdf.

Clarke, L., Jiang, K., Akimoto, K., Babiker, M., Blanford, G., Fisher-Vanden, K., Hourcade, J.-C., Krey, V., Kriegler, E., Löschel, A., McCollum, D., Paltsev, S., Rose, S., Shukla, P.R., Tavoni, M., van der Zwaan, B.C.C., van Vuuren, D.P., 2014. Assessing transformation pathways. In: Edenhofer, O., Pichs-Madruga, R., Sokona, Y., Farahani, E., Kadner, S., Seyboth, K., Adler, A., Baum, I., Brunner, S., Eickemeier, P., Kriemann, B., Savolainen, J., Schlömer, S., von Stechow, C., Zwickel, T., Minx, J.C. (Eds.), Climate Change 2014: Mitigation of Climate Change. Contribution of Working Group III to the Fifth Assessment Report of the Intergovernmental Panel on Climate Change. Cambridge University Press, Cambridge, United Kingdom and New York, NY, USA.

Challinor, A.J., et al., 2014. A meta-analysis of crop yield under climate change and adaptation. Nat. Clim. Change 4 (4), 287–291. http://dx.doi.org/10.1038/NCLIMATE2153.

Christensen, J.H., Krishna Kumar, K., Aldrian, E., An, S.-I., Cavalcanti, I.F.A., de Castro, M., Dong, W., Goswami, P., Hall, A., Kanyanga, J.K., Kitoh, A., Kossin, J., Lau, N.-C., Renwick, J., Stephenson, D.B., Xie, S.-P., Zhou, T., 2013. Climate phenomena and their relevance for future regional climate change. In: Stocker, T.F., Qin, D., Plattner, G.-K., Tignor, M., Allen, S.K., Boschung, J., Nauels, A., Xia, Y., Bex, V., Midgley, P.M. (Eds.), Climate Change 2013: The Physical Science Basis. Contribution of Working Group I to the Fifth Assessment Report of the Intergovernmental Panel on Climate Change. Cambridge University Press, Cambridge, United Kingdom and New York, NY, USA.

Church, J.A., Clark, P.U., Cazenave, A., Gregory, J.M., Jevrejeva, S., Levermann, A., Merrifield, M.A., Milne, G.A., Nerem, R.S., Nunn, P.D., Payne, A.J., Pfeffer, W.T., Stammer, D., Unnikrishnan, A.S., 2013. Sea level change. In: Stocker, T.F., Qin, D., Plattner, G.-K., Tignor, M., Allen, S.K., Boschung, J., Nauels, A., Xia, Y., Bex, V., Midgley, P.M. (Eds.), Climate Change 2013: The Physical Science Basis. Contribution of Working Group I to the Fifth Assessment Report of the Intergovernmental Panel on Climate Change. Cambridge University Press, Cambridge, United Kingdom and New York, NY, USA.

Collins, M., Knutti, R., Arblaster, J., Dufresne, J.-L., Fichefet, T., Friedlingstein, P., Gao, X., Gutowski, W.J., Johns, T., Krinner, G., Shongwe, M., Tebaldi, C., Weaver, A.J., Wehner, M., 2013. In: Stocker, T.F., Qin, D., Plattner, G.-K., Tignor, M., Allen, S.K., Boschung, J., Nauels, A., Xia, Y., Bex, V., Midgley, P.M. (Eds.), Long-term Climate Change: Projections, Commitments and Irreversibility. In: Climate Change 2013: The Physical Science Basis. Contribution of Working Group I to the Fifth Assessment Report of the Intergovernmental Panel on Climate Change. Cambridge University Press, Cambridge, United Kingdom and New York, NY, USA.

Crespo, O., Hachigonta, S., Tadross, M., 2011. Sensitivity of southern African maize yields to the definition of sowing dekad in a changing climate. Clim. Change 106, 267–283.

Deryng, D., Elliott, J., Ruane, A.C., Folberth, C., Müller, C., Pugh, T.A.M., Schmid, E., Boote, K.J., Conway, D., Gerten, D., Jones, J.W., Khabarov, N., Olin, S., Schaphoff, S., Yang, H., Rosenzweig, C., 2016. Regional disparities in the beneficial effects of rising CO2 concentrations on crop water productivity. Nat. Clim. Change 6 (8), 786–790. http://dx.doi.org/10.1038/nclimate2995.

Diffenbaugh, N.S., Singh, D., Mankin, J.S., 2018. Unprecedented climate events: historical changes, aspirational targets, and national commitments. Sci. Adv. 4, eaao3354.

Donatelli, M., Magarey, R.D., Bregaglio, S., Willocquet, L., Whish, J.P.M., Savary, S., 2017. Modelling the impacts of pests and diseases on agricultural systems. Agric. Syst. 155, 213–224. http://dx.doi.org/10.1016/j.agsy.2017.01.019.

Elliott, J., Deryng, D., Müller, C., Frieler, K., Konzmann, M., Gerten, D., Glotter, M., Flörke, M., Wada, Y., Best, N., Eisner, S., Fekete, B.M., Folberth, C., Foster, I., Gosling, S.N., Haddeland, I., Khabarov, N., Ludwig, F., Masaki, Y., Olin, S., Rosenzweig, C., Ruane, A.C., Satoh, Y., Schmid, E., Stacke, T., Tang, Q., Wisser, D., 2014. Constraints and potentials of future irrigation water availability on agricultural production under climate change. Proc. Natl. Acad. Sci. U. S. A. 111 (9), 3239–3244. http://dx.doi.org/10.1073/pnas.1222474110.

Elliott, J., Müller, C., Deryng, D., Chryssanthacopoulos, J., Boote, K.J., Büchner, M., Foster, I., Glotter, M., Heinke, J., Iizumi, T., Izaurralde, R.C., Mueller, N.D., Ray, D.K., Rosenzweig, C., Ruane, A.C., Sheffield, J., 2015. The global gridded crop model intercomparison: data and modeling protocols for phase 1 (v1.0). Geosci. Model. Dev. 8, 261–277. http://dx.doi.org/10.5194/gmd-8-261-2015.

Eyring, V., Bony, S., Meehl, G.A., Senior, C.A., Stevens, B., Stouffer, R.J., Taylor, K.E., 2016. Overview of the coupled model intercomparison project phase 6 (CMIP6) experimental design and organization. Geosci. Model. Dev. 9, 1937–1958. http://dx.doi.org/10.5194/gmd-9-1937-2016.

FAO, 2016. The State of Food and Agriculture: Climate Change. 194 pages. Available online at:. Agriculture and Food Security. http://www.fao.org/3/a-i6030e.pdf.

Faye, B., et al., 2018. What does 1.5 versus 2.0 °C of global warming mean for cereal yields in the West African Sudan Savannah? Environ. Res. Lett. 13, 034014. http://dx.doi.org/10.1088/1748-9326/aaab40.

Flato, G., Marotzke, J., Abiodun, B., Braconnot, P., Chou, S.C., Collins, W., Cox, P., Driouech, F., Emori, S., Eyring, V., Forest, C., Gleckler, P., Guilyardi, E., Jakob, C., Kattsov, V., Reason, C., Rummukainen, M., 2013. Evaluation of climate models. In: Stocker, T.F., Qin, D., Plattner, G.-K., Tignor, M., Allen, S.K., Boschung, J., Nauels, A., Xia, Y., Bex, V., Midgley, P.M. (Eds.), Climate Change 2013: The Physical Science Basis. Contribution of Working Group I to the Fifth Assessment Report of the Intergovernmental Panel on Climate Change. Cambridge University Press, Cambridge, United Kingdom and New York, NY, USA. 741–882. http://dx.doi.org/10.1017/CBO9781107415324.020.

Fleisher, D.H., Condori, B., Quiroz, R., Alva, A., Asseng, S., Barreda, C., Bindi, M., Boote, K.J., Ferrise, R., Franke, A.C., Govindakrishnan, P.M., Harahagazwe, D., Hoogenboom, G., Naresh Kumar, S., Merante, P., Nendel, C., Olesen, J.E., Parker, P.S., Raes, D., Raymundo, R., Ruane, A.C., Stockle, S., Supit, I., Vanuytrecht, E., Wolf, J., Woli, P., 2017. A potato model inter-comparison across varying climates and productivity levels. Glob. Change Biol. 23 (3), 1258–1281. http://dx.doi.org/10.1111/gcb.13411.

Glotter, M., Elliott, J., 2016. Simulating US agriculture in a modern dust bowl drought. Nat. Plants 3, 16193. http://dx.doi.org/10.1038/nplants.2016.193.

Hansen, J., Sato, M., Hearty, P., Ruedy, R., Kelley, M., Masson-Delmotte, V., Russell, G., Tselioudis, G., Cao, J., Rignot, E., Velicogna, I., Tormey, B., Donovan, B., Kandiano, E., von Schuckmann, K., Kharecha, P., LeGrande, A.N., Bauer, M., Lo, K.-M., 2016. Ice melt, sea level rise and superstorms: evidence from paleoclimate data, climate modeling, and modern observations that 2 °C global warming could be dangerous. Atmos. Chem. Phys. 16, 3761–3812.

Hartmann, D.L., Klein Tank, A.M.G., Rusticucci, M., Alexander, L.V., Brönnimann, S., Charabi, Y., Dentener, F.J., Dlugokencky, E.J., Easterling, D.R., Kaplan, A., Soden, B.J., Thorne, P.W., Wild, M., Zhai, P.M., 2013. . Observations: atmosphere and surface. In: Stocker, T.F., Qin, D., Plattner, G.-K., Tignor, M., Allen, S.K., Boschung, J., Nauels, A., Xia, Y., Bex, V., Midgley, P.M. (Eds.), Climate Change 2013: The Physical Science Basis. Contribution of Working Group I to the Fifth Assessment Report of the

Intergovernmental Panel on Climate Change. Cambridge University Press, Cambridge, United Kingdom and New York, NY, USA.
Hatfield, J.L., Boote, K.J., Kimball, B.A., Ziska, L.H., Izaurralde, R.C., Ort, D., Thomson, A.M., Wolfe, D., 2011. Climate impacts on agriculture: implications for crop production. Agronomy 103 (2). http://dx.doi.org/10.2134/agronj2010.0303.
Hempel, S., Frieler, K., Warszawski, L., Shewe, J., Piontek, F., 2013. A trend-preserving bias correction—the ISI-MIP approach. Earth Syst. Dynam. 4, 219–236.
Howden, S.M., Soussana, J.F., Tubiello, F.N., Chhetri, N., Dunlop, M., Meinke, H., 2007. Adapting agriculture to climate change. Proc. Natl. Acad. Sci. U. S. A. 104, 19691–19696. http://dx.doi.org/10.1073/pnas.0701890104.
IPCC, 2013. Summary for policymakers. In: Stocker, T.F., Qin, D., Plattner, G.-K., Tignor, M., Allen, S.K., Boschung, J., Nauels, A., Xia, Y., Bex, V., Midgley, P.M. (Eds.), Climate Change 2013: The Physical Science Basis. Contribution of Working Group I to the Fifth Assessment Report of the Intergovernmental Panel on Climate Change. Cambridge University Press, Cambridge, United Kingdom and New York, NY, USA.
IPCC, 2014. Summary for policymakers. In: Field, C.B., Barros, V.R., Dokken, D.J., Mach, K.J., Mastrandrea, M.D., Bilir, T.E., Chatterjee, M., Ebi, K.L., Estrada, Y.O., Genova, R.C., Girma, B., Kissel, E.S., Levy, A.N., MacCracken, S., Mastrandrea, P.R., White, L.L. (Eds.), Climate Change 2014: Impacts, Adaptation, and Vulnerability. Part A: Global and Sectoral Aspects. Contribution of Working Group II to the Fifth Assessment Report of the Intergovernmental Panel on Climate Change. Cambridge University Press, Cambridge, United Kingdom and New York, NY, USA, pp. 1–32.
Iizumi, T., Luo, J.-J., Challinor, A.J., Sakurai, G., Yokozawa, M., Sakuma, H., Brown, M.E., Yamagata, T., 2014. Impacts of El Niño Southern Oscillation on the global yields of major crops. Nat. Commun. 5 (3712). http://dx.doi.org/10.1038/ncomms4712.
Karmalker, A.V., Bradley, R.S., 2017. Consequences of global warming of 1.5 °C and 2 °C for regional temperature and precipitation changes in the contiguous United States. PLoS One 12. http://dx.doi.org/10.1371/journal.pone.0168697.
Kimball, B.A., 2016. Crop responses to elevated CO2 and interactions with H2O, N, and temperature. Curr. Opin. Plant Biol. 31, 36–43.
Kriegler, E., Edmonds, J., Hallegatte, S., Ebi, K.L., Kram, T., Riahi, K., Winkler, H., van Vuuren, D.P., 2014. A new scenario framework for climate change research: the concept of shared climate policy assumptions. Clim. Change 122, 401–414. http://dx.doi.org/10.1007/s10584-013-0971-5.
Lau, K.-M., Kim, K.-M., 2006. Observational relationships between aerosol and Asian monsoon rainfall, and circulation. Geophys. Res. Lett. 33, L21810. http://dx.doi.org/10.1029/2006GL027546.
Li, T., Hasegawa, T., Yin, X., Zhu, Y., Boote, K., Adam, M., Bregaglio, S., Buis, S., Confalonieri, R., Fumoto, T., Gaydon, D., Marcaida III, M., Nakagawa, H., Oriol, P., Ruane, A.C., Ruget, F., Singh, B., Singh, U., Tang, L., Tao, F., Wilkens, P., Yoshida, H., Zhang, Z., Bouman, B., 2015. Uncertainties in predicting rice yield by current crop models under a wide range of climatic conditions. Glob. Change Biol. 21 (3), 1328–1341. http://dx.doi.org/10.1111/gcb.12758.
Lobell, D.B., Hammer, G.L., McLean, G., Messina, C., Roberts, M.J., Schlenker, W., 2013. The critical role of extreme heat for maize production in the United States. Nat. Clim. Change 3, 497.
Lobell, D.B., Bänziger, M., Magorokosho, C., Vivek, B., 2011. Nonlinear heat effects on African maize as evidenced by historical yield trials. Nat. Clim. Change 1, 42–45.
Lopez, A., Suckling, E.B., Smith, L.A., 2014. Robustness of pattern scaled climate change scenarios for adaptation decision support. Clim. Change 122, 555–566. http://dx.doi.org/10.1007/s10584-013-1022-y.
Maiorano, A., Martre, P., Asseng, S., Ewert, F., Müller, C., Rötter, R., Ruane, A.C., Semenov, M., Wallach, D., Wang, E., Alderman, P., Kassie, B., Biernath, C., Basso, B., Cammarano, D., Challinor, A.J., Doltra, J., Dumont, B., Eyshi Rezaei, E., Gayler, S., Kersebaum, K.C., Kimball, B.A., Koehler, A.K., Liu, B., O'Leary, G.J., Olesen, J.E., Ottman, M.J., Priesack, E., Reynolds, M.P., Stratonovitch, P., Streck, T., Thorburn, P.J., Waha, K., Wall, G.W., White, J.W., Zhao, Z., Zhu, Y., 2017. Crop model improvement reduces the uncertainty of the response to temperature of multi-model ensembles. Field Crops Res. 202, 5–20. http://dx.doi.org/10.1016/j.fcr.2016.05.001.
McDermid, S.P., Mearns, L.O., Ruane, A.C., 2017. Representing agriculture in earth system models: approaches and priorities for development. J. Adv. Model. Earth Syst. 9 (5), 2230–2265. http://dx.doi.org/10.1002/2016MS000749.
Mitchell, D., AchutaRao, K., Allen, M., Bethke, I., Beyerle, U., Ciavarella, A., Forster, P.M., Fuglestvedt, J., Gillett, N., Haustein, K., Ingram, W., Iversen, T., Kharin, V., Klingaman, N., Massey, N., Fischer, E., Schleussner, C.-F., Scinocca, J., Seland, Ø., Shiogama, H., Shuckburgh, E., Sparrow, S., Stone, D., Uhe, P., Wallom, D., Wehner, M., Zaaboul, R., 2017. Half a degree additional warming, prognosis and projected impacts (HAPPI): background and experimental design. Geosci. Model. Dev. 10, 571–583.
Morice, C.P., Kennedy, J.J., Rayner, N.A., Jones, P.D., 2012. Quantifying uncertainties in global and regional temperature change using an ensemble of observational estimates: the HadCRUT4 dataset. J. Geophys. Res. 117, D08101. http://dx.doi.org/10.1029/2011JD017187.
Moss, R.H., Edmonds, J.A., Hibbard, K.A., Manning, M.R., Rose, S.K., van Vuuren, D.P., Carter, T.R., Emori, S., Kainuma, M., Kram, T., Meehl, G.A., Mitchell, J.F.B., Nakicenovic, N., Riahi, K., Smith, S.J., Stouffer, R.J., Thomson, A.M., Weyant, J.P., Wilbanks, T.J., 2010. The next generation of scenarios for climate change research and assessment. Nature 463 (7282), 747–756. http://dx.doi.org/10.1038/nature08823.
Müller, C., Elliott, J., Chryssanthacopoulos, J., Arneth, A., Balkovič, J., Ciais, P., Deryng, D., Folberth, C., Glotter, M., Hoek, S., Iizumi, T., Izaurralde, R.C., Jones, C., Khabarov, N., Lawrence, P., Liu, W., Olin, S., Pugh, T.A.M., Ray, D., Reddy, A., Rosenzweig, C., Ruane, A.C., Sakurai, G., Schmid, E., Skalsky, R., Song, C.X., Wang, X., de Wit, A., Yang, H., 2017. Global gridded crop model evaluation: benchmarking, skills, deficiencies and implications. Geosci. Model. Dev. 10, 1403–1422. http://dx.doi.org/10.5194/gmd-10-1403-2017.
O'Leary, G.J., Christy, B., Nuttall, J., Huth, N., Cammarano, D., Stöckle, C., Basso, B., Shcherbak, I., Fitzgerald, G., Luo, Q., Farre-Codina, I., Palta, J., Asseng, S., 2015. Response of wheat growth, grain yield and water use to elevated CO2 under a free-air CO2 enrichment (FACE) experiment and modelling in a semi-arid environment. Glob. Change Biol. 21, 2670–2686.
O'Neill, B.C., Kriegler, E., Riahi, K., Ebi, K.L., Hallegatte, S., Cater, T.R., Mathur, R., van Vuuren, D.P., 2014. A new scenario framework for climate change research: the concept of shared socioeconomic pathways. Clim. Change 122, 387–400. http://dx.doi.org/10.1007/s10584-013-0905-2.
Pendergrass, A.G., Hartmann, D.L., 2014. Changes in the distribution of rain frequency and intensity in response to global warming. J. Climate 27, 8372–8383. http://dx.doi.org/10.1175/JCLI-D-14-00183.1.
Pirttioja, N., Carter, T., Fronzek, S., Bindi, M., Hoffmann, H., Palosuo, T., Ruiz-Ramos, M., Tao, F., Acutis, M., Asseng, S., Baranowski, P., Basso, B., Bodin, P., Buis, S., Cammarano, D., Deligios, P., Destain, M.-F., Dumont, B., Ewert, R., Ferrise, R., François, L., Gaiser, T., Hlavinka, P., Jacquemin, I., Kersebaum, K.C., Kollas, C., Krzyszczak, J., Lorite, I.J., Minet, J., Minguez, M.I., Montesino, M., Moriondo, M., Müller, C., Nendel, C., Öztürk, I., Perego, A., Rodríguez, A., Ruane, A.C., Ruget, F., Sanna, M., Semenov, M.A., Slawinski, C., Stratonovitch, P., Supit, I., Waha, K., Wang, E., Wu, L., Zhao, Z., Rötter, R.P., 2015. A crop model ensemble analysis of temperature and precipitation effects on wheat yield across a European transect using impact response surfaces. Clim. Res. 65, 87–105. http://dx.doi.org/10.3354/cr01322.
Porter, J.R., Xie, L., Challinor, A.J., Cochrane, K., Howden, S.M., Iqbal, M.M., Lobell, D.B., Travasso, M.I., 2014. Food security and food production systems. In: Field, C.B., Barros, V.R., Dokken, D.J., Mach, K.J., Mastrandrea, M.D., Bilir, T.E., Chatterjee, M., Ebi, K.L., Estrada, Y.O., Genova, R.C., Girma, B., Kissel, E.S., Levy, A.N., MacCracken, S., Mastrandrea, P.R., White, L.L. (Eds.), Climate Change 2014: Impacts, Adaptation, and Vulnerability. Part A: Global and Sectoral Aspects. Contribution of Working Group II to the Fifth Assessment Report of the Intergovernmental Panel on Climate Change. Cambridge University Press, Cambridge, United Kingdom and New York, NY, USA, pp. 485–533.
Ramanathan, V., Chung, C., Kim, D., Bettge, T., Buja, L., Kiehl, J.T., Washington, W.M., Fu, Q., Sikka, D.R., Wild, M., 2005. Atmospheric brown clouds: impacts on South Asian climate and hydrological cycle. PNAS 102 (15), 5326–5333.
Rickards, L., Howden, S.M., 2012. Transformational adaptation: agriculture and climate change. Crop Pasture Sci. 63, 240–250. http://dx.doi.org/10.1071/CP11172. 2012.
Rind, D., Chin, M., Feingold, G., Streets, D., Kahn, R.A., Schwartz, S.E., Yu, H., 2009. Modeling the effects of aerosols on climate, in atmospheric aerosol properties and impacts on climate. In: Chin, M., Kahn, R.A., Schwartz, S.E. (Eds.), Aerosol Properties and Their Impacts on Climate, U.S. Climate Change Science Program Synthesis and Assessment Product 2.3. National Aeronautics and Space Administration, pp. 64–97.
Rohde, R., Muller, R., Jacobsen, R., Perlmutter, S., Rosenfeld, A., Wurtele, J., Curry, J., Wickham, C., Mosher, S., 2013. Berkeley earth temperature averaging process. Geoinfor. Geostat: An. Overv. 1 (2). http://dx.doi.org/10.4172/2327-4581.1000103.
Rosenzweig, C., Tubiello, F.N., 2007. Adaptation and mitigation strategies in agriculture: an analysis of potential synergies. Mitig. Adapt. Strat. Glob. Change 12, 855–873. http://dx.doi.org/10.1007/s11027-007-9103-8.
Rosenzweig, C., Jones, J.W., Hatfield, J.L., Ruane, A.C., Boote, K.J., Thorburn, P., Antle, J.M., Nelson, G.C., Porter, C., Janssen, S., Asseng, S., Basso, B., Ewert, F., Wallach, D., Baigorria, G., Winter, J.M., 2013. The agricultural model intercomparison and improvement project (AgMIP): protocols and pilot studies. Agric. For. Meteorol. 170, 166–182. http://dx.doi.org/10.1016/j.agrformet.2012.09.011.
Rosenzweig, C., Elliott, J., Deryng, D., Ruane, A.C., Müller, C., Arneth, A., Boote, K.J., Folberth, C., Glotter, M., Khabarov, N., Neumann, K., Piontek, F., Pugh, T.A.M., Schmid, E., Stehfest, E., Yang, H., Jones, J.W., 2014. Assessing agricultural risks of climate change in the 21st century in a global gridded crop model intercomparison. Proc. Natl. Acad. Sci. U. S. A. 111 (9), 3268–3273. http://dx.doi.org/10.1073/pnas.1222463110.
Rosenzweig, C., Jones, J.W., Hatfield, J.L., Antle, J.M., Ruane, A.C., Mutter, C.Z., 2015. The agricultural model intercomparison and improvement project: phase I activities by a global community of science. In: In: Rosenzweig, C., Hillel, D. (Eds.), The Handbook of Climate Change and Agroecosystems: The Agricultural Model Intercomparison and Improvement Project (AgMIP), vol. 3. Imperial College Press, pp. 3–24. http://dx.doi.org/10.1142/9781783265640_0001. ICP Series on Climate Change Impacts, Adaptation, and Mitigation.
Rosenzweig, C., Antle, J., Elliott, J., 2016. Assessing Impacts of Climate Change on Food Security Worldwide 97 Eoshttp://dx.doi.org/10.1029/2016EO047387.
Rosenzweig, et al., 2018. Coordinating AgMIP data and models across global and regional scales for 1.5 °C and 2.0 °C assessments. Phil. Trans. R. Soc. A, 20160455. http://dx.doi.org/10.1098/rsta.2016.0455.
Ruane, A.C., McDermid, S.P., 2017. Selection of a representative subset of global climate models that captures the profile of regional changes for integrated climate impacts assessment. Earth Perspect. 4 (1). http://dx.doi.org/10.1186/s40322-017-0036-4.
Ruane, A.C., Major, D.C., Yu, W.H., Alam, M., Hussain, S.G., Khan, A.S., Hassan, A., Al Hossain, B.M.T., Goldberg, R., Horton, R.M., Rosenzweig, C., 2013. Multi-factor impact analysis of agricultural production in Bangladesh with climate change. Glob. Environ. Change A 23, 336–350. http://dx.doi.org/10.1016/j.gloenvcha.2012.09.001.
Ruane, A.C., McDermid, S., Rosenzweig, C., Baigorria, G.A., Jones, J.W., Romero, C.C., Cecil, L.D., 2014. Carbon–temperature–water change analysis for peanut production under climate change: a prototype for the AgMIP coordinated climate-crop modeling project (C3MP). Glob. Change Biol. 20, 394–407. http://dx.doi.org/10.1111/gcb.12412.
Ruane, A.C., Goldberg, R., Chryssanthacopoulos, J., 2015a. Climate forcing datasets for agricultural modeling: merged products for gap-filling and historical climate series

estimation. Agric. For. Meteorol. 200, 233–248. http://dx.doi.org/10.1016/j.agrformet.2014.09.016.

Ruane, A.C., Winter, J.M., McDermid, S.P., Hudson, N.I., 2015b. AgMIP climate datasets and scenarios for integrated assessment. In: In: Rosenzweig, C., Hillel, D. (Eds.), The Handbook of Climate Change and Agroecosystems: The Agricultural Model Intercomparison and Improvement Project Integrated Crop and Economic Assessments, Part 1, vol. 3. Imperial College Press, pp. 45–78. http://dx.doi.org/10.1142/9781783265640_0003. ICP Series on Climate Change Impacts, Adaptation, and Mitigation.

Ruane, A.C., Rosenzweig, C., Asseng, S., Boote, K.J., Elliott, J., Ewert, F., Jones, J.W., Martre, P., McDermid, S., Müller, C., Snyder, A., Thorburn, P.J., 2017. An AgMIP framework for improved agricultural representation in IAMs. Environ. Res. Lett. http://dx.doi.org/10.1088/1748-9326/aa8da6. in press.

Ruane, A.C., Antle, J., Elliott, J., Folberth, C., Hoogenboom, G., Mason-D'Croz, D., Müller, C., Porter, C.H., Phillips, M., Raymundo, R., Sands, R., Valdivia, R., White, J., Wiebe, K., Rosenzweig, C., 2018. Biophysical and economic implications for agriculture of +1. 5 and +2 .0 C global warming using AgMIP Coordinated Global and Regional Assessments. Clim. Res in press. https://doi.org/10.3354/cr01520.

Savary, S., Ficke, A., Aubertot, J.-N., Hollier, C., 2012. Crop losses due to diseases and their implications for global food production losses and food security. Food Sec. 4 (2). http://dx.doi.org/10.1007/s12571-012-0200-5.

Schleussner, C.-F., Deryng, D., Müller, C., Elliott, J., Saeed, F., Folberth, C., Liu, W., Wang, X., Pugh, T.A.M., Thiery, W., Seneviratne, S.I., Rogelj, J., 2018. Crop productivity changes in 1. 5 °C and 2 °C worlds under climate sensitivity uncertainty. Env. Res. Lett. 13, 064007. http://dx.doi.org/10.1088/1748-9326/aab63b.

SRES, 2000. In: Nakicenovic, N., Alcamo, J., Grubler, A., Riahi, K., Roehrl, R.A., Rogner, H.-H., Victor, N. (Eds.), Special Report on Emissions Scenarios, A Special Report of Working Group III of the Intergovernmental Panel on Climate Change. Cambridge University Press, Cambridge, UK 599 pages.

Tadross, M., Suarez, P., Lotsch, A., Hachigonta, S., Mdoka, M., Unganai, L., Lucio, F., Kamdonyo, D., Muchinda, M., 2009. Growing-season rainfall and scenarios of future change in southeast Africa: implications for cultivating maize. Clim. Res. 40, 147–169.

Taylor, K.E., Stouffer, R.J., Meehl, G.A., 2012. An overview of CMIP5 and the experiment design. Bull. Am. Meteorol. Soc. 93 (4), 485–498. http://dx.doi.org/10.1175/BAMSD-11-00094.1.

Tebaldi, C., Arblaster, J.M., 2014. Pattern scaling: its strengths and limitations, and an update on the latest model simulations. Clim. Change 122 (459). http://dx.doi.org/10.1007/s10584-013-1032-9.

Trenberth, K., 2011. Changes in precipitation with climate change. Clim. Res. 47, 123–138. http://dx.doi.org/10.3354/cr00953.

UNFCCC, 2015. Adoption of the Paris Agreement. 32 pages. Available online at:. United Nations Framework Convention on Climate Change. http://unfccc.int/resource/docs/2015/cop21/eng/l09r01.pdf.

van Vuuren, D., van Sluisveld, M., Hof, A.F., 2015. Implications of Long-Term Scenarios for Medium-Term Targets (2050). PBL Netherlands Environmental Assessment Agency publication number 1871. 30 pages. Available online at:. http://www.pbl.nl/sites/default/files/cms/publicaties/pbl-2015-implications-for-long-term-scenarios-for-medium-term-targets-2050_01871.pdf.

Wiebe, K., Lotze-Campen, H., Sands, R., Tabeau, A., van der Mensbrugghe, D., Biewald, A., Bodirsky, B., Islam, S., Kavallari, A., Mason-D'Croz, D., Müller, C., Popp, A., Robertson, R., Robinson, S., van Meiji, H., Willenbockel, D., 2015. Climate change impacts on agriculture in 2050 under a range of plausible socioeconomic and emissions scenarios. Environ. Res. Lett. 10, 085010. http://dx.doi.org/10.1088/1748-9326/10/8/085010.

WMO, 1989. Calculation of Monthly and Annual 30-Year Standard Normals (WCDP928 No.10, WMO-TD/No.341). World Meteorological Organization, Geneva.

Yadav, S.S., Redden, R., Hatfield, J.L., Lotze-Campen, H., Hall, A.J., 2011. Crop Adaptation to Climate Change. 632 pages. John Wiley & Sons, Oxford, United Kingdom. http://dx.doi.org/10.1002/9780470960929.

You, L., Wood-Sichra, U., Fritz, S., Guo, Z., See, L., Koo, J., 2014. Spatial Production Allocation Model (SPAM) 2005 v2.0. Available online at:. http://mapspam.info.

Zhao, C., Liu, B., Piao, S., Wang, X., Lobell, D.B., Huang, Y., Huang, M., Yao, Y., Bassu, S., Ciais, P., Durand, J.-L., Elliott, J., Ewert, F., Janssens, I.A., Li, T., Lin, E., Liu, Q., Martre, P., Müller, C., Peng, S., Peñuelas, J., Ruane, A.C., Wallach, D., Wang, T., Wu, D., Liu, Z., Zhu, Y., Zhu, Z., Asseng, S., 2017. Temperature increase reduces global yields of major crops in four independent estimates. Proc. Natl. Acad. Sci. U. S. A. 114 (35), 9326–9331. http://dx.doi.org/10.1073/pnas.1701762114.

Zhang, H.-M., Huang, B., Lawrimore, J., Menne, M., Smith, T.M., 2017. NOAA Global Surface Temperature Dataset (NOAAGlobalTemp), Version 4.0 Global Anomalies and Index Data. NOAA National Centers for Environmental Informationhttp://dx.doi.org/10.7289/V5FN144H. (Accessed 7 March 2017).